

Decentralized Frank-Wolfe Algorithm for Convex and Non-convex Problems

Hoi-To Wai, Jean Lafond, Anna Scaglione, Eric Moulines ^{*†}

December 9, 2024

Abstract

Decentralized optimization algorithms have received much attention due to the recent advances in network information processing. However, conventional decentralized algorithms based on projected gradient descent are incapable of handling high dimensional constrained problems, as the projection step becomes computationally prohibitive to compute. To address this problem, this paper adopts a projection-free optimization approach, a.k.a. the Frank-Wolfe (FW) or conditional gradient algorithm. We first develop a decentralized FW (DeFW) algorithm from the classical FW algorithm. The convergence of the proposed algorithm is studied by viewing the decentralized algorithm as an *inexact* FW algorithm. Using a diminishing step size rule and letting t be the iteration number, we show that the DeFW algorithm's convergence rate is $\mathcal{O}(1/t)$ for convex objectives; is $\mathcal{O}(1/t^2)$ for strongly convex objectives with the optimal solution in the interior of the constraint set; and is $\mathcal{O}(1/\sqrt{t})$ towards a stationary point for smooth but non-convex objectives. We then show that a consensus-based DeFW algorithm meets the above guarantees with two communication rounds per iteration. Furthermore, we demonstrate the advantages of the proposed DeFW algorithm on low-complexity robust matrix completion and communication efficient sparse learning. Numerical results on synthetic and real data are presented to support our findings.

1 Introduction

Recently, algorithms for tackling high-dimensional optimizations have been sought for the ‘big-data’ challenge [3]. As these data/measurements are dispersed over clouds of networked machines, it is important to consider *decentralized* algorithms that can allow the agents/machines to co-operate and leverage the aggregated computation power [4].

This paper considers decentralized algorithm for tackling a constrained optimization problem with N agents:

$$\min_{\boldsymbol{\theta} \in \mathbb{R}^d} F(\boldsymbol{\theta}) \text{ s.t. } \boldsymbol{\theta} \in \mathcal{C}, \text{ where } F(\boldsymbol{\theta}) := \frac{1}{N} \sum_{i=1}^N f_i(\boldsymbol{\theta}), \quad (1)$$

*The work of H.-T. Wai is supported by NSF CCF-1553746, NSF CCF-1531050 and J. Lafond by Direction Générale de l'Armement and the labex LMH (ANR-11-LABX-0056-LMH). Preliminary versions of this work are presented at ICASSP 2016 [1] and GlobalSIP 2016 [2].

†H.-T. Wai and A. Scaglione are with the School of Electrical, Computer and Energy Engineering, Arizona State University, Tempe, AZ 85281, USA. E-mails: {htwai, Anna.Scaglione}@asu.edu. J. Lafond was with Institut Mines-Telecom, Telecom ParisTech, CNRS LTCI, Paris, France. Email: lafond.jean@gmail.com. E. Moulines is with CMAP, Ecole Polytechnique, Palaiseau, France. Email: eric.moulines@polytechnique.edu.

and $f_i(\boldsymbol{\theta})$ is a continuously differentiable (possibly non-convex) function held by the i th agent and \mathcal{C} is a closed and bounded convex set in \mathbb{R}^d . Typically, the function $f_i(\boldsymbol{\theta})$ models the loss function over the private data held by agent i , and \mathcal{C} corresponds to a regularization constraint imposed on the optimization variable $\boldsymbol{\theta}$ such as sparsity or low rank of an array of values. Problem (1) covers a number of applications in control theory, signal processing and machine learning, including system identification [5], matrix completion [6] and sparse learning [7, 8].

To tackle (1), the agents communicate on a network described as a graph $G = (V, E)$, where $V = \{1, \dots, N\}$ is the set of agents and $E \subseteq V \times V$ describes the connectivity. As G is not fully connected, it is useful to apply decentralized algorithms that relies on *near-neighbor* information exchanges. In light of this, various authors have proposed to tackle (1) through decentralized algorithms that are built on the average consensus protocol [9, 10]. For example, [11–18] studied the decentralized gradient methods; [19, 20] considered the Newton-type methods; [21–25] considered the decentralized primal-dual algorithms. [26, 27] are built on the successive convex approximation framework. The convergence properties of these algorithms were investigated extensively, especially for convex objectives [4, 12–25]; for non-convex objectives, a few recent results can be found in [11, 25–29]. However, most prior work are *projection*-based such that each iteration of the above algorithms necessitates a projection step onto the constraint set \mathcal{C} , or solving a sub-problem with similar complexity. While the projection step entails a modest complexity for problems with moderate dimension, it may become computationally prohibitive for high dimensional problems, thereby rendering the above methods impractical for our scenario of interest.

To address the issue above, this paper focuses on a decentralized *projection-free* algorithm. We extend the Frank-Wolfe (FW) algorithm [30] to operate with near-neighbor information exchange, leading to a decentralized FW (DeFW) algorithm. The FW (a.k.a. conditional gradient) algorithm has been recently popularized due to its efficacy in handling high-dimensional constrained problems. Examples of its applications include optimal control [31], matrix completion [32], image and video colocation [33], electric vehicle charging [34] and traffic assignment [35]; see the overview article [36]. From the algorithmic perspective, the FW algorithm replaces the costly projection step in PG based algorithms with a constrained linear optimization, which often admits an efficient solution. In a centralized setting, the convergence of FW algorithm has been studied for convex problems [30, 36], yet little is known for non-convex problems [37–39].

Our contributions are as follows. We first describe abstractly the DeFW algorithm as a variation of the FW algorithm with *inexact* iterates and gradients. We then analyze its convergence — for convex objectives, the sub-optimality (of objective values) of the iterates produced by the proposed algorithm is shown to converge as $\mathcal{O}(1/t)$ with t being the iteration number, and is $\mathcal{O}(1/t^2)$ for strongly convex objectives when the optimal solution is in the interior of \mathcal{C} ; for non-convex objectives, we demonstrate that the proposed algorithm has limit points that are stationary points of (1), and they can be found at the rate of $\mathcal{O}(\sqrt{1/t})$. We then show that a consensus-based implementation of the proposed algorithm with fixed number of communication rounds of near-neighbor information exchanges achieves all the above guarantees. To our knowledge, this is the first decentralized FW algorithm. Moreover, our convergence rate in the non-convex setting is comparable to that of a *centralized* projected gradient method [40]. Lastly, we present examples on communication-efficient LASSO and decentralized matrix completion.

The rest of this paper is organized as follows. Section 2 develops the DeFW algorithm. We summarize the main theoretical results of convergence for convex and non-convex objective functions. A consensus-based implementation of the DeFW algorithm will then be presented in Section 3. Ap-

plications of the DeFW algorithm are discussed in Section 4. Finally, Section 5 presents numerical results to support our findings.

1.1 Notations & Mathematical Preliminaries

For any $d \in \mathbb{N}$, we define $[d]$ as the set $\{1, \dots, d\}$. We use boldfaced lower-case letters to denote vectors and boldfaced upper-case letters to denote matrices. For a vector \mathbf{x} (or a matrix \mathbf{X}), the notation $[\mathbf{x}]_i$ (or $[\mathbf{X}]_{i,j}$) denotes its i th element (or (i, j) th element). The vectorization of a matrix $\mathbf{X} \in \mathbb{R}^{m_1 \times m_2}$ is denoted by $\text{vec}(\mathbf{X}) = [\mathbf{x}_1; \mathbf{x}_2; \dots; \mathbf{x}_{m_2}] \in \mathbb{R}^{m_1 m_2}$ such that \mathbf{x}_i is the i th column of \mathbf{X} . The vector $\mathbf{e}_i \in \mathbb{R}^d$ is the i th unit vector such that $[\mathbf{e}_i]_j = 0$ for all $j \neq i$ and $[\mathbf{e}_i]_i = 1$. For some positive finite constants C_1, C_2, C_3 , $C_2 \leq C_3$ and non-negative functions $f(t), g(t)$, the notations $f(t) = \mathcal{O}(g(t))$, $f(t) = \Theta(g(t))$ indicate $f(t) \leq C_1 g(t)$, $C_2 g(t) \leq f(t) \leq C_3 g(t)$ for sufficiently large t , respectively.

Let \mathbf{E} be a Euclidean space embedded in \mathbb{R}^d and the Euclidean norm is denoted by $\|\cdot\|_2$. The binary operator $\langle \cdot, \cdot \rangle$ denotes the inner product on \mathbf{E} . In addition, \mathbf{E} is equipped with a norm $\|\cdot\|$ and the corresponding dual norm $\|\cdot\|_*$. Let G, L, μ be non-negative constants. Consider a function $f: \mathbb{R}^d \rightarrow \mathbb{R}$, the function f is G -Lipschitz if for all $\boldsymbol{\theta}, \boldsymbol{\theta}' \in \mathbf{E}$,

$$|f(\boldsymbol{\theta}) - f(\boldsymbol{\theta}')| \leq G \|\boldsymbol{\theta} - \boldsymbol{\theta}'\|; \quad (2)$$

the function f is L -smooth if for all $\boldsymbol{\theta}, \boldsymbol{\theta}' \in \mathbf{E}$,

$$f(\boldsymbol{\theta}) - f(\boldsymbol{\theta}') \leq \langle \nabla f(\boldsymbol{\theta}'), \boldsymbol{\theta} - \boldsymbol{\theta}' \rangle + \frac{L}{2} \|\boldsymbol{\theta} - \boldsymbol{\theta}'\|_2^2, \quad (3)$$

the above is equivalent to $\|\nabla f(\boldsymbol{\theta}') - \nabla f(\boldsymbol{\theta})\|_2 \leq L \|\boldsymbol{\theta}' - \boldsymbol{\theta}\|_2$; the function f is μ -strongly convex if for all $\boldsymbol{\theta}, \boldsymbol{\theta}' \in \mathbf{E}$,

$$f(\boldsymbol{\theta}) - f(\boldsymbol{\theta}') \leq \langle \nabla f(\boldsymbol{\theta}), \boldsymbol{\theta} - \boldsymbol{\theta}' \rangle - \frac{\mu}{2} \|\boldsymbol{\theta} - \boldsymbol{\theta}'\|_2^2; \quad (4)$$

moreover, f is convex if the above is satisfied with $\mu = 0$.

Consider Problem (1), its constraint set $\mathcal{C} \subseteq \mathbf{E}$ is convex and bounded with the diameter defined as:

$$\rho := \max_{\boldsymbol{\theta}, \boldsymbol{\theta}' \in \mathcal{C}} \|\boldsymbol{\theta} - \boldsymbol{\theta}'\|, \quad \bar{\rho} := \max_{\boldsymbol{\theta}, \boldsymbol{\theta}' \in \mathcal{C}} \|\boldsymbol{\theta} - \boldsymbol{\theta}'\|_2, \quad (5)$$

note that ρ is defined with respect to (w.r.t.) the norm $\|\cdot\|$ while $\bar{\rho}$ is defined w.r.t. the Euclidean norm. When the objective function F is μ -strongly convex with $\mu > 0$, the optimal solution to (1) is unique and denoted by $\boldsymbol{\theta}^*$, we also define

$$\delta := \min_{\mathbf{s} \in \partial \mathcal{C}} \|\mathbf{s} - \boldsymbol{\theta}^*\|_2, \quad (6)$$

where $\partial \mathcal{C}$ is the boundary set of \mathcal{C} . If $\delta > 0$, the solution $\boldsymbol{\theta}^*$ is in the interior of \mathcal{C} .

2 Decentralized Frank-Wolfe (DeFW)

We develop the decentralized Frank-Wolfe (DeFW) algorithm from the classical FW algorithm [30]. Let $t \in \mathbb{N}$ be the iteration number and the initial point $\boldsymbol{\theta}_0 \in \mathcal{C}$ is feasible. Recall the definition

Algorithm 1 Decentralized Frank-Wolfe (DeFW).

1: **Input:** Initial point $\boldsymbol{\theta}_1^i$ for $i = 1, \dots, N$.

2: **for** $t = 1, 2, \dots$ **do**

3: *Consensus:* approximate the average iterate:

$$\bar{\boldsymbol{\theta}}_t^i \leftarrow \text{NetAvg}_t^i(\{\boldsymbol{\theta}_t^j\}_{j=1}^N), \quad \forall i \in [N].$$

4: *Aggregating:* approximate the average gradient:

$$\overline{\nabla}_t^i F \leftarrow \text{NetAvg}_t^i(\{\nabla f_j(\bar{\boldsymbol{\theta}}_t^j)\}_{j=1}^N), \quad \forall i \in [N].$$

5: *Frank-Wolfe Step:* update

$$\boldsymbol{\theta}_{t+1}^i \leftarrow (1 - \gamma_t)\bar{\boldsymbol{\theta}}_t^i + \gamma_t \mathbf{a}_t^i \quad \text{where } \mathbf{a}_t^i \in \arg \min_{\mathbf{a} \in \mathcal{C}} \langle \overline{\nabla}_t^i F, \mathbf{a} \rangle,$$

for all agent $i \in [N]$ and $\gamma_t \in (0, 1]$ is a step size.

6: **end for**

7: **Return:** $\bar{\boldsymbol{\theta}}_{t+1}^i, \forall i \in [N]$.

$F(\boldsymbol{\theta}) := (1/N) \sum_{i=1}^N f_i(\boldsymbol{\theta})$, the *centralized* FW algorithm for problem (1) proceeds by:

$$\mathbf{a}_{t-1} \in \arg \min_{\mathbf{a} \in \mathcal{C}} \langle \nabla F(\boldsymbol{\theta}_{t-1}), \mathbf{a} \rangle, \quad (7a)$$

$$\boldsymbol{\theta}_t = \boldsymbol{\theta}_{t-1} + \gamma_{t-1}(\mathbf{a}_{t-1} - \boldsymbol{\theta}_{t-1}), \quad (7b)$$

where $\gamma_{t-1} \in (0, 1]$ is a step size to be determined. Observe that $\boldsymbol{\theta}_t$ is a convex combination of $\boldsymbol{\theta}_{t-1}$ and \mathbf{a}_{t-1} which are both feasible, therefore $\boldsymbol{\theta}_t \in \mathcal{C}$ as \mathcal{C} is a convex set. When the step size is chosen as $\gamma_t = 2/(t+1)$, the FW algorithm is known to converge at a rate of $\mathcal{O}(1/t)$ if F is L -smooth and convex [36]. A main feature of the FW algorithm is that the linear optimization¹ (LO) (7a) can be solved more efficiently than computing a projection, leading to a *projection-free* algorithm. At the end of this section, we will illustrate a few examples of \mathcal{C} with efficient LO computations.

Our next endeavor is to extend the FW algorithm to a decentralized setting via mimicking (7) with only near-neighbor information exchanges. Doing so requires replacing the centralized gradient/iterate $\nabla F(\boldsymbol{\theta}_t)$, $\boldsymbol{\theta}_t$ in (7) with local approximations, as similar to the strategy in [14, 24].

In the following, we offer a high-level description of the proposed DeFW algorithm and discuss the convergence properties of it. Details regarding the implementation will be postponed to Section 3. Let $\boldsymbol{\theta}_t^i$ denotes an auxiliary iterate kept by agent i at iteration t . Define the average iterate:

$$\bar{\boldsymbol{\theta}}_t := N^{-1} \sum_{i=1}^N \boldsymbol{\theta}_t^i \quad (8)$$

and the local iterate $\bar{\boldsymbol{\theta}}_t^i$ as an approximation of the average iterate above, also kept by agent i . We require $\bar{\boldsymbol{\theta}}_t^i$ to track $\bar{\boldsymbol{\theta}}_t$ with an increasing accuracy. Let $\{\Delta p_t\}_{t \geq 1}$ be a non-negative, decreasing sequence with $\Delta p_t \rightarrow 0$, we assume

¹Notice that (7a) is a convex optimization problem with a linear objective.

Assumption 1 ($\{\Delta p_t\}_{t \geq 1}$) For all $t \geq 1$, it holds that

$$\max_{i \in [N]} \|\bar{\boldsymbol{\theta}}_t^i - \bar{\boldsymbol{\theta}}_t\|_2 \leq \Delta p_t. \quad (9)$$

To compute (7a), ideally each agent has to access the *global gradient*, $\nabla F(\bar{\boldsymbol{\theta}}_t)$. However, just the local function $f_i(\cdot)$ is available and agent i can only compute the local gradient $\nabla f_i(\bar{\boldsymbol{\theta}}_t^i)$. Therefore, we also need to track the average gradient,

$$\overline{\nabla_t F} := N^{-1} \sum_{j=1}^N \nabla f_j(\bar{\boldsymbol{\theta}}_t^j), \quad (10)$$

by the local approximation $\overline{\nabla_t^i F}$. Note that $\overline{\nabla_t^i F}$ is close to $\nabla F(\bar{\boldsymbol{\theta}}_t)$ when each of the function $f_i(\boldsymbol{\theta})$ is smooth and $\bar{\boldsymbol{\theta}}_t^i$ is close to $\bar{\boldsymbol{\theta}}_t$. Let $\{\Delta d_t\}_{t \geq 1}$ be a non-negative, decreasing sequence with $\Delta d_t \rightarrow 0$, we assume:

Assumption 2 ($\{\Delta d_t\}_{t \geq 1}$) For all $t \geq 1$, it holds that

$$\max_{i \in [N]} \|\overline{\nabla_t^i F} - \overline{\nabla_t F}\|_2 \leq \Delta d_t. \quad (11)$$

Naturally, from the local approximation $\overline{\nabla_t^i F}$, the i th agent can compute the update direction $\mathbf{a}_t^i = \arg \min_{\mathbf{a} \in \mathcal{C}} \langle \overline{\nabla_t^i F}, \mathbf{a} \rangle$ and update $\boldsymbol{\theta}_{t+1}^i$ similarly as in (7b). To summarize, a sketch of the DeFW algorithm can be found in Algorithm 1.

Under Assumptions 1-2, for each agent i , line 5 in Algorithm 1 can be regarded as performing an *inexact* FW update on $\bar{\boldsymbol{\theta}}_t$, whose convergence can be characterized below. For convex objective functions, we have:

Theorem 1 Set the step size as $\gamma_t = 2/(t+1)$. Suppose that each of f_i is convex and L -smooth. Let C_p and C_g be two positive constants. Under Assumptions 1-2 [$\Delta p_t = C_p/t$, $\Delta d_t = C_g/t$], we have

$$F(\bar{\boldsymbol{\theta}}_t) - F(\boldsymbol{\theta}^*) \leq \frac{8\bar{\rho}(C_g + LC_p) + 2L\bar{\rho}^2}{t+1}, \quad (12)$$

for all $t \geq 1$, where $\boldsymbol{\theta}^*$ is an optimal solution to (1). Furthermore, if F is μ -strongly convex and the optimal solution $\boldsymbol{\theta}^*$ lies in the interior of \mathcal{C} , i.e., $\delta > 0$ (cf. (6)), we have

$$F(\bar{\boldsymbol{\theta}}_t) - F(\boldsymbol{\theta}^*) \leq \frac{(4\bar{\rho}(C_g + LC_p) + L\bar{\rho}^2)^2}{2\delta^2\mu} \cdot \frac{9}{(t+1)^2}, \quad (13)$$

for all $t \geq 1$.

The proof can be found in Appendix A. We remark that $\bar{\boldsymbol{\theta}}_t$ is always feasible. For strongly convex objective functions, the conditions (12), (13) imply that the sequence $\{\bar{\boldsymbol{\theta}}_t\}_{t \geq 1}$ converges to an optimal solution of (1). Furthermore, as the consensus error, $\max_{i \in [N]} \|\bar{\boldsymbol{\theta}}_t^i - \bar{\boldsymbol{\theta}}_t\|_2$, decay to zero (cf. Assumption 1), the local iterates $\{\bar{\boldsymbol{\theta}}_t^i\}_{t \geq 1}$ share similar convergence guarantee as $\{\bar{\boldsymbol{\theta}}_t\}_{t \geq 1}$.

For non-convex objective functions, we study the convergence of the FW/duality gap:

$$g_t := \max_{\boldsymbol{\theta} \in \mathcal{C}} \langle \nabla F(\bar{\boldsymbol{\theta}}_t), \bar{\boldsymbol{\theta}}_t - \boldsymbol{\theta} \rangle. \quad (14)$$

From the definition, when $g_t = 0$, the iterate $\bar{\boldsymbol{\theta}}_t$ will be a stationary point to (1). Thus we may regard g_t as a measure of the stationarity of the iterate $\bar{\boldsymbol{\theta}}_t$. Also, define the set of stationary point to (1) as:

$$\mathcal{C}^* = \{\boldsymbol{\theta} \in \mathcal{C} : \max_{\boldsymbol{\theta} \in \mathcal{C}} \langle \nabla F(\boldsymbol{\theta}), \boldsymbol{\theta} - \boldsymbol{\theta} \rangle = 0\}. \quad (15)$$

We consider the following technical assumption:

Assumption 3 *The set \mathcal{C}^* is non-empty. Moreover, the function $F(\boldsymbol{\theta})$ takes a finite number of values over \mathcal{C}^* , i.e., the set $F(\mathcal{C}^*) = \{F(\boldsymbol{\theta}) : \boldsymbol{\theta} \in \mathcal{C}^*\}$ is finite.*

Verifying Assumption 3 may be hard in practice. Meanwhile, it is reasonable to assume that (1) has a finite number of stationary points since the set \mathcal{C} is bounded. In the latter case, Assumption 3 is satisfied. We now have:

Theorem 2 *Set the step size as $\gamma_t = 1/t^\alpha$ for some $\alpha \in (0, 1]$. Suppose each of f_i is L -smooth and G -Lipschitz (possibly non-convex). Let C_p, C_g be two positive constants. Under Assumption 1-2 [$\Delta p_t = C_p/t^\alpha, \Delta d_t = C_g/t^\alpha$], it holds that:*

1. for all $T \geq 6$ that are even, if $\alpha \in [0.5, 1)$,

$$\min_{t \in [T/2+1, T]} g_t \leq \frac{1}{T^{1-\alpha}} \cdot \frac{1-\alpha}{(1-(2/3)^{1-\alpha})} \cdot \left(G\rho + (L\bar{\rho}^2/2 + 2\bar{\rho}(C_g + LC_p)) \log 2 \right); \quad (16)$$

if $\alpha \in (0, 0.5)$,

$$\min_{t \in [T/2+1, T]} g_t \leq \frac{1}{T^\alpha} \cdot \frac{1-\alpha}{(1-(2/3)^{1-\alpha})} \cdot \left(G\rho + \frac{(L\bar{\rho}^2/2 + 2\bar{\rho}(C_g + LC_p))(1-(1/2)^{1-2\alpha})}{1-2\alpha} \right). \quad (17)$$

2. additionally, under Assumption 3 and $\alpha \in (0.5, 1]$, the sequence of objective values $\{F(\bar{\boldsymbol{\theta}}_t)\}_{t \geq 1}$ converges, $\{\bar{\boldsymbol{\theta}}_t\}_{t \geq 1}$ has limit points and each limit point is in \mathcal{C}^* .

The proof can be found in Appendix B. Note that setting $\alpha = 0.5$ gives the quickest convergence rate of $\mathcal{O}(1/\sqrt{T})$. It is worth mentioning that our results are novel compared to prior work on non-convex FW even in a centralized setting ($N = 1, \Delta p_t = 0, \Delta d_t = 0$). For instance, [37] requires that the local minimizer is unique; [38] gives the same convergence rate but uses an adaptive step size. We remark that the local iterates $\{\bar{\boldsymbol{\theta}}_t^i\}_{t \geq 1}$ share similar convergence property as $\{\bar{\boldsymbol{\theta}}_t\}_{t \geq 1}$ due to Assumption 1.

Lastly, we survey some relevant examples of the constraint set \mathcal{C} where the LO in the DeFW algorithm (cf. line 5 in Algorithm 1) can be computed efficiently:

1. When \mathcal{C} is the ℓ_1 ball, $\mathcal{C} = \{\boldsymbol{\theta} \in \mathbb{R}^d : \|\boldsymbol{\theta}\|_1 \leq R\}$,

$$\mathbf{a}_t^i = -R \cdot \mathbf{e}_k, \text{ where } k \in \arg \max_{j \in [d]} |\overline{[\nabla_t^i F]}_j|. \quad (18)$$

The solution above amounts to finding the coordinate index of $\overline{[\nabla_t^i F]}$ with the maximum magnitude. Importantly, this solution is only 1-sparse. Consequently, the t th iterate $\bar{\boldsymbol{\theta}}_t$ will be at most tN -sparse. The worst-case complexity of computing \mathbf{a}_t^i is $\mathcal{O}(d)$; in comparison, the worst-case complexity for the projection into an ℓ_1 ball is $\mathcal{O}(d \log d)^2$.

²There exists a randomized, accelerated algorithm for projection in [41] with an *expected* complexity of $\mathcal{O}(d)$.

2. When \mathcal{C} is the trace norm ball, $\mathcal{C} = \{\boldsymbol{\theta} \in \mathbb{R}^{m_1 \times m_2} : \|\boldsymbol{\theta}\|_{\sigma,1} \leq R\}$, where $\|\boldsymbol{\theta}\|_{\sigma,1}$ is the sum of the singular values of $\boldsymbol{\theta}$. Let $\mathbf{u}_1, \mathbf{v}_1$ be the top-1 left/right singular vector of $\overline{\nabla_t^i F}$, we have

$$\mathbf{a}_t^i = -R \cdot \mathbf{u}_1 \mathbf{v}_1^\top. \quad (19)$$

Importantly, at a target solution accuracy of δ , the top singular vectors can be computed with a complexity of $\mathcal{O}(\max\{m_1, m_2\} \log(1/\delta))$ using the power/Lanczos method if $\|\text{vec}(\overline{\nabla_t^i F})\|_0 = \mathcal{O}(\max\{m_1, m_2\})$. In comparison, the projection onto the trace norm ball requires a complexity of $\mathcal{O}(\max\{m_1 m_2^2, m_2 m_1^2\} \log(1/\delta))$ for computing the full SVD of an $m_1 \times m_2$ matrix [42].

For more examples of \mathcal{C} with efficient LO computations, the interested readers are referred to [36] for an overview.

3 Consensus-based DeFW algorithm

This section demonstrates how an average consensus (AC) based scheme can generate local approximations $\hat{\boldsymbol{\theta}}_t^i, \overline{\nabla_t^i F}$ at the desirable sub-linear accuracies (cf. Assumptions 1-2) using as few as two communication rounds per iteration.

Specifically, the following discussions are based on the static AC [9,10]. While the exact details are left for a future work, we believe that it is possible to extend our protocol to a time varying network's setting. We consider an undirected graph $G = (V, E)$ and assign a non-negative, symmetric *weighted adjacency matrix* $\mathbf{W} \in \mathbb{R}_+^{N \times N}$ that describes the local communication between the N agents. The matrix satisfies $W_{ij} := [\mathbf{W}]_{ij} > 0$ iff $(i, j) \in E$ and it is doubly stochastic, i.e., $\mathbf{W}\mathbf{1} = \mathbf{W}^\top \mathbf{1} = \mathbf{1}$. Moreover,

Assumption 4 *The second largest (in magnitude) eigenvalue of \mathbf{W} is strictly less than one, i.e., $|\lambda_2(\mathbf{W})| < 1$.*

The existence of such matrix \mathbf{W} is guaranteed if G is connected. For each round of the AC update, the agents take a weighted average of the values from its neighbors according to \mathbf{W} . We now state the following fact regarding \mathbf{W} .

Fact 1 *Let $\mathbf{x}_1, \dots, \mathbf{x}_N \in \mathbb{R}^d$ be a set of vectors and $\mathbf{x}_{\text{avg}} := N^{-1} \sum_{i=1}^N \mathbf{x}_i$ be their average. Suppose \mathbf{W} is a doubly stochastic, non-negative matrix. The output after performing one round of AC update:*

$$\bar{\mathbf{x}}_i = \sum_{j=1}^N W_{ij} \cdot \mathbf{x}_j \quad (20)$$

must satisfy

$$\sqrt{\sum_{i=1}^N \|\bar{\mathbf{x}}_i - \mathbf{x}_{\text{avg}}\|_2^2} \leq |\lambda_2(\mathbf{W})| \cdot \sqrt{\sum_{i=1}^N \|\mathbf{x}_i - \mathbf{x}_{\text{avg}}\|_2^2}, \quad (21)$$

where $\lambda_2(\mathbf{W})$ is the second largest eigenvalue of \mathbf{W} .

The fact above can be verified from linear algebra. Together with Assumption 4, the above implies that each AC update (20) moves the vectors closer to the average \mathbf{x}_{avg} . Repeatedly applying (21) shows the well known fact that AC computes the average \mathbf{x}_{avg} at a linear rate.

Let us consider the near-neighbor computation of $\bar{\theta}_t^i$ in line 3 of Algorithm 1. Here, the *consensus step* is computed by:

$$\bar{\theta}_t^i = \sum_{j=1}^N W_{ij} \cdot \theta_t^j, \quad (22)$$

i.e., we apply one round of the AC update. Since $W_{ij} = 0$ if $(i, j) \notin E$, the above operation is achievable by information exchanges with the near-neighbors of agent i .

Now, for some $\alpha \in (0, 1]$, we define $t_0(\alpha)$ as the smallest integer such that

$$\lambda_2(\mathbf{W}) \leq \left(\frac{t_0(\alpha)}{t_0(\alpha) + 1} \right)^\alpha \cdot \frac{1}{1 + (t_0(\alpha))^{-\alpha}}. \quad (23)$$

Notice that $t_0(\alpha)$ is upper bounded by:

$$t_0(\alpha) \leq \lceil (|\lambda_2(\mathbf{W})|^{-1/(1+\alpha)} - 1)^{-1} \rceil, \quad (24)$$

which is finite under Assumption 4. The following lemma can be easily proven:

Lemma 1 *Set the step size $\gamma_t = 1/t^\alpha$ in the DeFW algorithm for some $\alpha \in (0, 1]$, then $\bar{\theta}_t^i$ in (22) satisfies Assumption 1:*

$$\max_{i \in [N]} \|\bar{\theta}_t^i - \bar{\theta}_t\|_2 \leq \Delta p_t = C_p/t^\alpha, \quad \forall t \geq 1, \quad (25)$$

$$C_p := (t_0(\alpha))^\alpha \cdot \sqrt{N\bar{\rho}}. \quad (26)$$

The proof is postponed to Appendix C, which relies on the observation that θ_t^i is a convex combination of $\bar{\theta}_{t-1}^i$ and \mathbf{a}_{t-1}^i . In particular, $\bar{\theta}_{t-1}^i$ is already $\mathcal{O}(1/(t-1)^\alpha)$ -close to the network average from the last iteration and the update direction \mathbf{a}_{t-1}^i is weighted by a decaying step size γ_{t-1} .

In comparison to what we were able to establish above, the near-neighbor computation of $\overline{\nabla}_t^i F$ in line 4 of the DeFW algorithm is less straightforward. Unlike the computation of $\bar{\theta}_t$, computing $N^{-1} \sum_{i=1}^N \nabla f_i(\bar{\theta}_t^i)$ to an accuracy of $\mathcal{O}(1/t^\alpha)$ by only communicating the local gradient $\nabla f_i(\bar{\theta}_t^i)$ requires $\sim \log t$ rounds of updates when the AC protocol is employed. The main issue is that the local gradient $\nabla f_i(\bar{\theta}_t^i)$ computed by the i th agent is different from the local gradient computed at the other agent, even when $\bar{\theta}_t^i$ is close to $\bar{\theta}_t^j$ for $j \neq i$.

We propose an approach that is inspired by the fast stochastic average gradient (SAGA) method [43] which re-uses the gradient approximation $\overline{\nabla}_{t-1}^i F$ from the last iteration³. Define the following surrogate of local gradient at iteration t :

$$\nabla_t^i F := \overline{\nabla}_{t-1}^i F + \nabla f_i(\bar{\theta}_t^i) - \nabla f_i(\bar{\theta}_{t-1}^i), \quad (27)$$

for all $i \in [N]$. When $t = 1$, we set $\nabla_1^i F = \nabla f_i(\bar{\theta}_1^i)$. We now apply the AC update to the gradient surrogate. In line 4 of Algorithm 1, the *aggregating* step is computed by:

$$\overline{\nabla}_t^i F = \sum_{j=1}^N W_{ij} \cdot \nabla_t^j F, \quad (28)$$

i.e., using just one round of AC update on $\nabla_t^i F$. Below we show that the average gradient is preserved by $\overline{\nabla}_t^i F$. Moreover, $\overline{\nabla}_t^i F$ has an approximation error similar to Lemma 1:

³After the submission, the authors notice that a similar technique is adopted in [13, 18, 27] under the name of ‘gradient tracking’ for various decentralized methods. We provide a rate analysis with non-asymptotic constants.

Lemma 2 Set the step size $\gamma_t = 1/t^\alpha$ in the DeFW algorithm for some $\alpha \in (0, 1]$. Suppose that each of f_i is L -smooth, $\bar{\theta}_t^i$ is updated according to (22), then $\overline{\nabla_t^i F}$ in (28) satisfies

$$N^{-1} \sum_{i=1}^N \nabla_t^i F = N^{-1} \sum_{i=1}^N \nabla f_i(\bar{\theta}_t^i), \quad \forall t \geq 1, \quad (29)$$

and Assumption 2:

$$\max_{i \in [N]} \|\overline{\nabla_t^i F} - \overline{\nabla_t F}\|_2 \leq \Delta d_t = C_g/t^\alpha, \quad \forall t \geq 1, \quad (30)$$

$$C_g := (t_0(\alpha))^\alpha \cdot 2\sqrt{N}(2C_p + \bar{\rho})L. \quad (31)$$

The proof can be found in Appendix D. Similar intuition as in Lemma 1 was used in the proof. In particular, we observe that $\overline{\nabla_t^i F}$ is a linear combination of $\overline{\nabla_{t-1}^i F}$ and $\nabla f_i(\bar{\theta}_t^i) - \nabla f_i(\bar{\theta}_{t-1}^i)$. The former is $\mathcal{O}(1/(t-1)^\alpha)$ -close to the average, and the latter decays to zero as enforced by the step size γ_t .

Finally, the conditions on $\Delta p_t, \Delta d_t$ necessitated by Theorem 1 & 2 can be satisfied by (22) & (28).

Corollary 1 Under Assumption 4, the results in Theorem 1 & 2 hold when line 3, line 4 in the DeFW algorithm (Algorithm 1) are computed by (22), (28) respectively.

In other words, the consensus-based DeFW algorithm converges for both convex and non-convex problems, while using a constant number of communication rounds per iteration.

As a final remark, recall from Theorem 2 that for non-convex objectives, the best rate of convergence can be achieved if we set $\alpha = 0.5$. However, from Lemma 1 & 2, we notice that the approximation error also decays the slowest when $\alpha = 0.5$. This presents a potential tradeoff in the choice of α . From our numerical experience, we find that setting $\alpha = 0.75$ yields a good performance in practice.

4 Applications

In this section, we study two applications of the DeFW algorithm to illustrate its flexibility and efficacy.

4.1 Example I: Decentralized Matrix Completion

Consider a setting when the network of agents obtain incomplete observations of a matrix θ_{true} of dimension $m_1 \times m_2$ with $m_1, m_2 \gg 0$. The i th agent has corrupted observations from the *training* set $\Omega_i \subset [m_1] \times [m_2]$ that are expressed as:

$$Y_{k,l} = [\theta_{\text{true}}]_{k,l} + Z_{k,l}, \quad \forall (k, l) \in \Omega_i. \quad (32)$$

To recover a low-rank θ_{true} , we consider the following trace-norm constrained matrix completion (MC) problem:

$$\min_{\theta \in \mathbb{R}^{m_1 \times m_2}} \sum_{i=1}^N \sum_{(k,l) \in \Omega_i} \tilde{f}_i([\theta]_{k,l}, Y_{k,l}) \quad \text{s.t.} \quad \|\theta\|_{\sigma,1} \leq R, \quad (33)$$

where $\tilde{f}_i: \mathbb{R}^2 \rightarrow \mathbb{R}$ is a loss function picked by agent i according to the observations he/she received. Notice that (33) is also related to the low rank subspace system identification problem described

in [5], where \mathbf{Y} with $[\mathbf{Y}]_{k,l} = Y_{k,l}$, $\boldsymbol{\theta}_{\text{true}}$ are modeled as the measured system response and the ground truth low rank response; also see [44] for a related work.

Similar MC problems have been considered in [45–48], where [45] studied a consensus-based optimization method similar to ours and [46–48] studied the parallel computation setting where the agents are working synchronously in a fully connected network. Compared to our approach, these work assume that the rank of $\boldsymbol{\theta}_{\text{true}}$ is known in advance and solve the MC problem via matrix factorization. In addition, [45,46] required that each local observation set Ω_i only have entries taken from a disjoint subset of the columns/rows only. Our approach does not have any restrictions above.

We consider two different observation models. When $Z_{k,l}$ is the i.i.d. Gaussian noise of variance σ_i^2 , we choose $\tilde{f}_i(\cdot, \cdot)$ to be the square loss function, i.e.,

$$\tilde{f}_i([\boldsymbol{\theta}]_{k,l}, Y_{k,l}) := (1/\sigma_i^2) \cdot (Y_{k,l} - [\boldsymbol{\theta}]_{k,l})^2. \quad (34)$$

This yields the classical MC problem in [6]. The next model considers the sparse+low rank matrix completion in [49], where the observations are contaminated with a sparse noise. Here, we model $Z_{k,l}$ as a *sparse* noise in the sense that there are a few number of entries in Ω_i where $Z_{k,l}$ is non-zero. We choose $\tilde{f}_i(\cdot, \cdot)$ to be the negated Gaussian loss, i.e.,

$$\tilde{f}_i([\boldsymbol{\theta}]_{k,l}, Y_{k,l}) := \left(1 - \exp\left(-\frac{([\boldsymbol{\theta}]_{k,l} - Y_{k,l})^2}{\sigma_i}\right)\right), \quad (35)$$

where $\sigma_i > 0$ controls the robustness to outliers for the data obtained at the i th agent. Here, $\tilde{f}_i(\cdot, \cdot)$ is a *smoothed* ℓ_0 loss [50] with enhanced robustness to outliers in the data. Notice that the resultant MC problem (33) is non-convex.

Note that (33) is a special case of problem (1) with \mathcal{C} being the trace-norm ball. The consensus-based DeFW algorithm can be applied on (33) directly. The projection-free nature of the DeFW algorithm leads to a low complexity implementation (33). Lastly, several remarks on the communication and storage cost of the DeFW algorithm are in order:

- The SAGA-like gradient surrogate $\nabla_t^i F$ (27) is supported only on $\cup_{i=1}^N \Omega_i$ since for all $i \in [N]$, the local gradient

$$\nabla f_i(\bar{\boldsymbol{\theta}}_t^i) = \sum_{(k,l) \in \Omega_i} \tilde{f}'_i([\bar{\boldsymbol{\theta}}_t^i]_{k,l}, Y_{k,l}) \cdot \mathbf{e}_k(\mathbf{e}'_l)^\top \quad (36)$$

is supported on Ω_i , where $\bar{\boldsymbol{\theta}}_t^i$ is defined in (22). In the above, \mathbf{e}_k (\mathbf{e}'_l) is the k th (l th) canonical basis vector for \mathbb{R}^{m_1} (\mathbb{R}^{m_2}) and $\tilde{f}'_i(\boldsymbol{\theta}, y)$ is the derivative of $\tilde{f}_i(\boldsymbol{\theta}, y)$ taken with respect to $\boldsymbol{\theta}$. Consequently, the average $\overline{\nabla_t^i F}$ is supported only on $\cup_{i=1}^N \Omega_i$. As $|\cup_{i=1}^N \Omega_i| \ll m_1 m_2$, the amount of information exchanged during the *aggregating* step (Line 4 in DeFW) is low.

- The update direction \mathbf{a}_t^i is a rank-one matrix composed of the top singular vectors of $\overline{\nabla_t^i F}$ (cf. (19)). Since every iteration in DeFW adds at most N distinct pair of singular vectors to $\bar{\boldsymbol{\theta}}_t$, the rank of $\bar{\boldsymbol{\theta}}_t^i$ is upper bounded by tN if we initialize by $\bar{\boldsymbol{\theta}}_0^i = \mathbf{0}$. We can reduce the communication cost in Line 3 in DeFW by exchanging these singular vectors. Note that $(tN) \cdot (m_1 + m_2)$ entries are stored/exchanged instead of $m_1 \cdot m_2$.
- When the agents are *only* concerned with predicting the entries of $\boldsymbol{\theta}_{\text{true}}$ in the subset $\Xi \subset [m_1] \times [m_2]$, instead of propagating the singular vectors as described above, the *consensus* step can be carried out by exchanging only the entries of $\boldsymbol{\theta}_{t+1}^i$ in $\Xi \cup (\cup_{i=1}^N \Omega_i)$ without affecting the operations of the DeFW algorithm. In this case, the storage/communication cost is $|\Xi \cup (\cup_{i=1}^N \Omega_i)|$.

4.2 Example II: Communication Efficient DeFW for LASSO

Let $(\mathbf{y}_i, \mathbf{A}_i)$ be the available data tuple at agent $i \in [N]$ such that $\mathbf{A}_i \in \mathbb{R}^{m \times d}$ and $\mathbf{y}_i \in \mathbb{R}^m$. The data \mathbf{y}_i is a corrupted measurement of an unknown parameter $\boldsymbol{\theta}_{\text{true}}$:

$$\mathbf{y}_i = \mathbf{A}_i \boldsymbol{\theta}_{\text{true}} + \mathbf{z}_i, \quad (37)$$

where $\mathbf{z}_i \sim \mathcal{N}(\mathbf{0}, \sigma^2 \mathbf{I})$ are independent noise vectors. Furthermore, we assume $m \ll d$ such that the matrix $\mathbf{A}_i^\top \mathbf{A}_i$ is rank-deficient. However, the parameter $\boldsymbol{\theta}_{\text{true}}$ is s -sparse such that $s = \|\boldsymbol{\theta}_{\text{true}}\|_0 \ll d$. This motivates us to consider the following distributed LASSO problem:

$$\min_{\boldsymbol{\theta} \in \mathbb{R}^d} \sum_{i=1}^N \frac{1}{2} \|\mathbf{y}_i - \mathbf{A}_i \boldsymbol{\theta}\|_2^2 \quad \text{s.t.} \quad \|\boldsymbol{\theta}\|_1 \leq R, \quad (38)$$

Notice that the above is a special case of (1) with $f_i(\boldsymbol{\theta}) = (1/2)\|\mathbf{y}_i - \mathbf{A}_i \boldsymbol{\theta}\|_2^2$ and \mathcal{C} is an ℓ_1 -ball in \mathbb{R}^d with radius R . We assume that (38) has an optimal solution $\boldsymbol{\theta}^*$ that is sparse. The settings above also correspond to identifying a linear system described by a sparse parameter $\boldsymbol{\theta}_{\text{true}}$, where $\mathbf{A}_i, \mathbf{y}_i$ are the input, output of the system, respectively; see [51] for a related formulation on the identification of switched linear systems.

A number of decentralized algorithms are easily applicable to (38). For example, the decentralized projected gradient (DPG) algorithm in [15] is described by — at iteration t ,

$$\boldsymbol{\theta}_{t+1}^{i,PG} = \mathcal{P}_{\mathcal{C}} \left(\sum_{j=1}^N W_{ij} \boldsymbol{\theta}_t^{j,PG} - \alpha_t \nabla f_i \left(\sum_{j=1}^N W_{ij} \boldsymbol{\theta}_t^{j,PG} \right) \right), \quad (39)$$

where $\alpha_t \in (0, 1]$ is a diminishing step size and W_{ij} is the weighted adjacency matrix described in Section 3. For convex problems, the DPG algorithm is shown to converge to an optimal solution $\boldsymbol{\theta}^*$ of (38) at a rate of $\mathcal{O}(1/\sqrt{t})$ [12].

Let us focus on the communication efficiency of the DPG algorithm, which is important when the network between agents is limited in bandwidth. To this end, we define the communication cost as the *number of non-zero real numbers exchanged per agent*. As seen from (39), at each iteration the i th agent exchanges its current iterate $\boldsymbol{\theta}_t^{i,PG}$ with the neighboring agents. From the computation step shown, $\boldsymbol{\theta}_t^{i,PG}$ may contain as high as $\mathcal{O}(d)$ non-zeros and the per-iteration communication cost will be $\mathcal{O}(d)$. Despite the high communication cost, the per-iteration computation complexity of (39) is also high, i.e., at $\mathcal{O}(d \log d)$ [41]. We notice that [7, 8] have considered distributed sparse recovery algorithm with focus on the communication efficiency. However, their algorithms are based on the iterative hard thresholding (IHT) formulation [52] that requires a-priori knowledge on the sparsity level of $\boldsymbol{\theta}_{\text{true}}$. Our consensus-based DeFW algorithm in Section 3 may also be applied directly to (38). However, similar issue as the DPG algorithm may arise during the *aggregating* step, since the gradient surrogate (27) may also have $\mathcal{O}(d)$ non-zeros. Lastly, another related work is [53] which applies coding to ‘compress’ the message exchanged in the consensus-based algorithms.

This section proposes a *sparsified DeFW algorithm* for solving (38). The modified algorithm applies a novel ‘sparsification’ procedure to reduce communication cost during the iterations, which is enabled by the structure of the DeFW algorithm. To describe the sparsified DeFW algorithm, we first argue that the *consensus step* in the consensus-based DeFW should remain unchanged as it already has a low communication cost. From (18) and (22), we see that $\boldsymbol{\theta}_t^i$ is at most $(t-1)N + 1$ -sparse since \mathbf{a}_t^i is always a 1-sparse vector⁴ (cf. (18)). As such, the communication cost of this step is bounded by tN .

⁴As pointed out by [36], this observation also leads to an interesting sparsity-accuracy trade-off when applying FW on ℓ_1 constrained problems.

Our focus is to improve the communication efficiency of *aggregating step*. Here, the key idea is that only the *largest magnitude coordinate* in $\overline{\nabla_t^i F}$ is sought when computing \mathbf{a}_t^i (cf. (18)). As long as the largest magnitude coordinate in $\overline{\nabla_t^i F}$ is preserved, the updates in the DeFW algorithm can remain unaffected. This motivates us to ‘sparsify’ the gradient information at each iteration before exchanging them with the neighboring agents. Let $\Omega_t \subseteq [d]$ be the coordinates of the gradient information to be exchanged at iteration t . The agents exchange the following gradient surrogate in lieu of (27):

$$\widehat{\nabla_t^i F} := (\nabla f_i(\bar{\boldsymbol{\theta}}_t^i)) \odot \mathbf{1}_{\Omega_t}, \quad \text{where } \mathbf{1}_{\Omega_t} = \sum_{k \in \Omega_t} \mathbf{e}_k, \quad (40)$$

and \odot denotes the Hadamard/element-wise product.

Let $\ell_t = \lceil C_l + \log(t)/\log|\lambda_2^{-1}(\mathbf{W})| \rceil$ where C_l is some finite constant and $\lambda_2(\mathbf{W})$ is the second largest eigenvalue of the weight matrix \mathbf{W} , the sparsified DeFW algorithm computes the approximate gradient average $\overline{\nabla_t^i F}$ in line 4 of Algorithm 1 by:

$$\overline{\nabla_t^i F} = \sum_{j=1}^N [\mathbf{W}^{\ell_t}]_{ij} \cdot \widehat{\nabla_t^j F}. \quad (41)$$

Note that (41) requires ℓ_t rounds of AC updates to be performed at iteration t , i.e., a logarithmically increasing number of rounds of AC updates. The update direction \mathbf{a}_t^i can then be computed by sorting the vector $\overline{\nabla_t^i F}$. As $\overline{\nabla_t^i F}$ is $|\Omega_t|$ -sparse, this update direction can be computed in $\mathcal{O}(|\Omega_t|)$ time.

We pick the coordinate set Ω_t in a decentralized manner. Consider the following decomposition:

$$\Omega_t = \bigcup_{i=1}^N \Omega_{t,i}, \quad (42)$$

where $\Omega_{t,i} \subset [d]$ is picked by agent i at iteration t . The coordinate set Ω_t needs to be known by all agents before (41). This can be achieved with low communication overhead, e.g., by forming a spanning tree on the graph G and broadcasting the required indices in Ω_t to all agents; see [54]. Set p_t as the maximum desirable cardinality of $\Omega_{t,i}$, agent i chooses the coordinate set using one of the following two schemes:

- (*Random coordinate*) Each agent selects $\Omega_{t,i}$ by picking p_t coordinates uniformly (with replacement) from $[d]$.
- (*Extreme coordinate*) Each agent selects $\Omega_{t,i}$ as the p_t largest magnitude coordinates of the vector $\nabla f_i(\bar{\boldsymbol{\theta}}_t^i)$.

For the random coordinate selection scheme, the following lemma shows that the gradient approximation error can be controlled at a desirable rate with an appropriate choice of p_t . Let $\xi_t := (1 - (1 - 1/d)^{p_t N})$, we have:

Lemma 3 *Set $\epsilon > 0$ and $\ell_t = \lceil C_l + \log(t)/\log|\lambda_2^{-1}(\mathbf{W})| \rceil$. Let $p_t \geq C_0 t$ for some $C_0 < \infty$. With probability at least $1 - \pi^2 \epsilon / 6$, the following holds for all $\boldsymbol{\theta} \in \mathcal{C}$:*

$$\left\| \xi_t^{-1} \overline{\nabla_t^i F} - \frac{1}{N} \sum_{i=1}^N \nabla f_i(\bar{\boldsymbol{\theta}}_t^i) \right\|_{\infty} = \mathcal{O}\left(\frac{d \sqrt{\log(t^2/\epsilon)}}{tN}\right), \quad (43)$$

for all $t \geq 1$ and $i \in [N]$.

The proof can be found in Appendix E. Note that the above is given in terms of $\xi_t^{-1}\overline{\nabla_t^i F}$ instead of $\overline{\nabla_t^i F}$. However, the result remains relevant as the LO (7a) in the DeFW algorithm is *scale invariant*, i.e., $\arg \min_{\mathbf{a} \in \mathcal{C}} \langle \overline{\nabla_t^i F}, \mathbf{a} \rangle = \arg \min_{\mathbf{a} \in \mathcal{C}} \langle \alpha \overline{\nabla_t^i F}, \mathbf{a} \rangle$ for any $\alpha > 0$. In other words, performing the FW step with $\overline{\nabla_t^i F}$ is equivalent to doing so with $\xi_t^{-1}\overline{\nabla_t^i F}$. As $\xi_t^{-1}\overline{\nabla_t^i F}$ is an $\mathcal{O}(1/t)$ approximation to $N^{-1} \sum_{j=1}^N \nabla f_j(\boldsymbol{\theta}_t^j)$, Assumption 2 is satisfied with $\Delta d_t = \mathcal{O}(1/t)$. Lastly, we conclude that

Corollary 2 *The sparsified DeFW algorithm using random coordinate selection, i.e., with line 3 & 4 in Algorithm 1 replaced by (22) & (41), respectively, generates iterates that satisfy the guarantees in Theorem 1 (with high probability). Under strong convexity and interior optimal point assumption, the communication complexity is $\mathcal{O}(N \cdot (1/\delta) \cdot \log(1/\delta))$ to reach a δ -optimal solution to (38).*

In the above, the first statement is a consequence of Lemma 3. The second statement can be verified by noting that reaching a δ -optimal solution requires $\mathcal{O}(1/\sqrt{\delta})$ iterations and the communication cost is $\mathcal{O}(Nt \log t)$ at iteration t , as the agents exchange an $\mathcal{O}(Nt)$ -sparse vector for $\Theta(\log t)$ times.

5 Numerical Experiments

We perform numerical experiments to verify our theoretical findings on the DeFW algorithm. The following discussions will focus on the two applications described in Section 4 using synthetic and real data. To simulate the decentralized optimization setting, we artificially construct a network of $N = 50$ agents, where the underlying communication network G is an Erdos-Renyi graph with connectivity of 0.1. For the AC steps (22), (28) & (41), the doubly stochastic matrix \mathbf{W} is calculated according to the Metropolis-Hastings rule in [55].

5.1 Decentralized Matrix Completion

This section considers the decentralized matrix completion problem, where the goal is to predict missing entries of an unknown matrix through corrupted partial measurements. We consider two datasets — the first dataset is synthetically generated where the unknown matrix $\boldsymbol{\theta}_{\text{true}}$ is rank- K and has dimensions of $m_1 \times m_2$; the matrix is generated as $\boldsymbol{\theta}_{\text{true}} = \sum_{i=1}^K \mathbf{y}_i \mathbf{x}_i^\top / K$ where $\mathbf{y}_i, \mathbf{x}_i$ have i.i.d. $\mathcal{N}(0, 1)$ entries and different settings of m_1, m_2, K will be experimented. The second dataset is the `movielens100k` dataset [56]. The unknown matrix $\boldsymbol{\theta}_{\text{true}}$ records the movie ratings of $m_1 = 943$ users on $m_2 = 1682$ movies; and a total of 10^5 entries in $\boldsymbol{\theta}_{\text{true}}$ are available as integers ranging from 1 to 5. The datasets are divided into training and testing sets and the mean square error (MSE) on the *testing set* is evaluated as:

$$\text{MSE} = |\Omega_{\text{test}}|^{-1} \sum_{(k,l) \in \Omega_{\text{test}}} |[\boldsymbol{\theta}_{\text{true}}]_{k,l} - [\hat{\boldsymbol{\theta}}]_{k,l}|^2, \quad (44)$$

where $\hat{\boldsymbol{\theta}}$ denotes the estimated $\boldsymbol{\theta}$ produced by the algorithm.

For the synthetic dataset, the training (testing) set contains 20% (80%) entries which are selected randomly. For `movielens100k`, the training (testing) set contains 80×10^3 (20×10^3) entries. The training data of the two datasets are equally partitioned into $N = 50$ parts; for `movielens100k`, each agent holds 1600 entries. We evaluate the performance of the proposed consensus-based DeFW algorithm applied to square loss and negated Gaussian loss, as described in Section 4.1. Unless otherwise specified, we fix the number of AC rounds applied at $\ell = 1$ such that the agents only exchange information once per iteration. As the negated Gaussian loss is non-convex, we set the

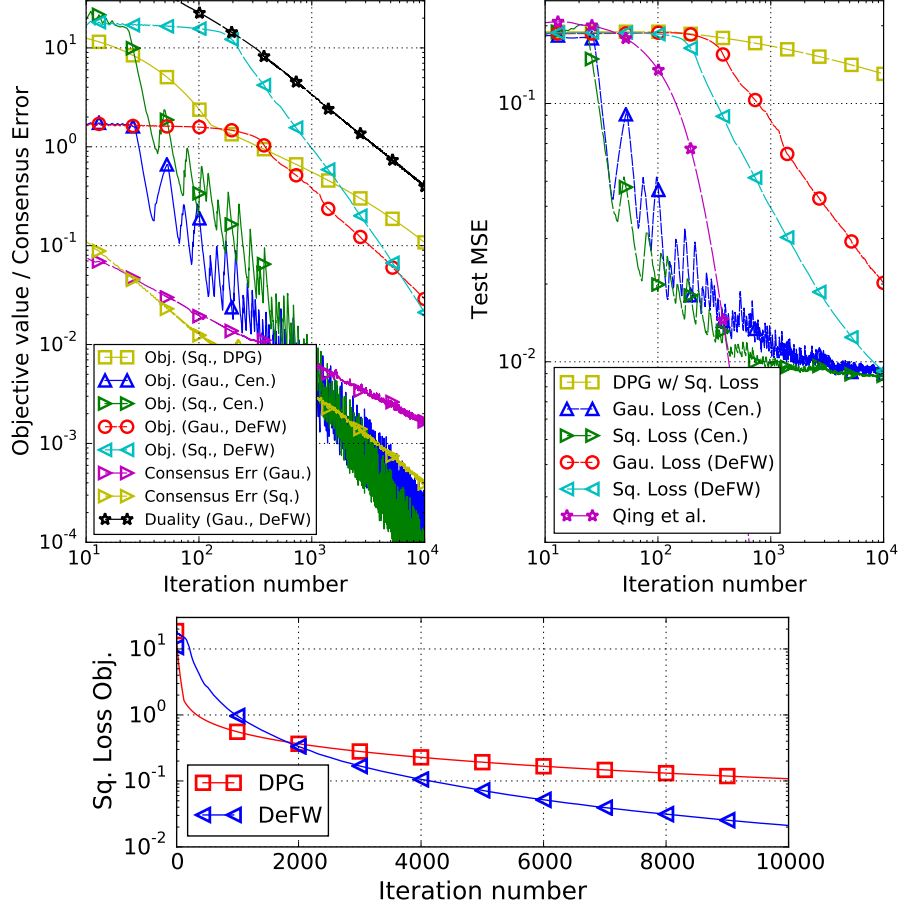


Figure 1: Results on noiseless synthetic data with $m_1 = 100, m_2 = 250$ and rank $K = 5$. (Top-Left) Objective value and consensus error of $\bar{\theta}_t^i$ against iteration number t , the objective values are evaluated by $F(\bar{\theta}_t)$. (Top-Right) Worst-case MSE (among agents) against iteration number on the testing set. (Bottom) Objective value (sq. loss) against iteration number t for DeFW and DPG. The legend ‘Gau.’, ‘Sq.’ denote the consensus-based DeFW algorithm applied to (33) with the negated Gaussian and square loss, respectively.

step size as $\gamma_t = t^{-0.75}$. The centralized FW algorithm for both losses will also be compared (cf. (7)); as well as the decentralized algorithm in [45] (labeled as ‘Qing et al.’) and the DPG algorithm [15] with step size set to $\alpha_t = 0.1N/(\sqrt{t} + 1)$ applied to square loss.

Our first example considers the noiseless synthetic dataset of problem dimension $m_1 = 100, m_2 = 250, K = 5$. The results are shown in Fig. 1. Here, for the DeFW/DPG algorithms, we set the trace-norm radius to $R = 1.2\|\theta_{\text{true}}\|_{\sigma,1}$; and the algorithm in [45] is supplied with the true rank K of θ_{true} . Notice that for this set of data, the minimum of (33) can be achieved by $\theta = \theta_{\text{true}} \in \mathcal{C}$ with a zero objective value. From the top-left plot, for the DeFW algorithm applied to the convex square loss function, we observe an $\mathcal{O}(1/t^2)$ trend for the objective values, corroborating with our analysis in Theorem 1; for the non-convex negated Gaussian loss function, the objective value and the FW/duality gap g_t also decay with t , the latter indicates the convergence to a stationary point. Moreover, the consensus error of $\bar{\theta}_t^i$ for DeFW applied to the two objective functions decay at the

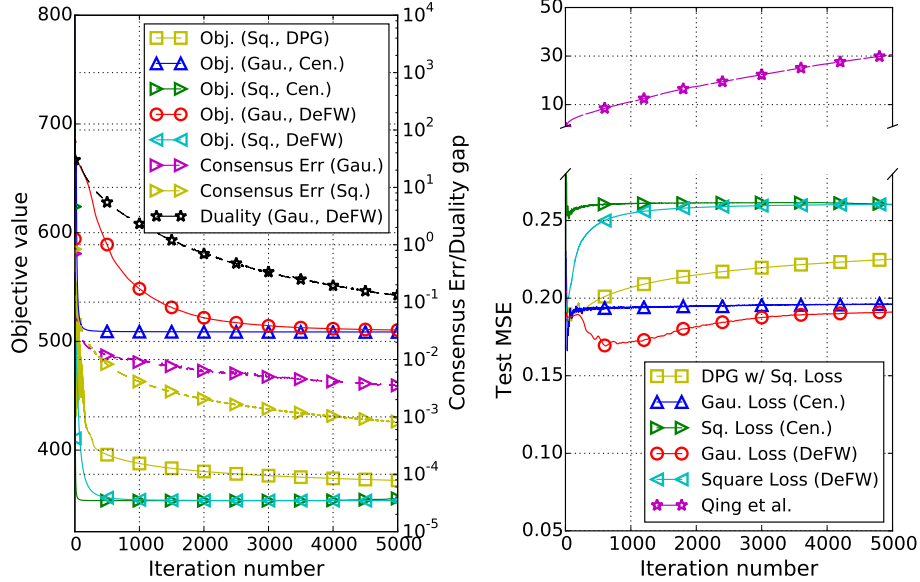


Figure 2: Results on sparse-noise contaminated synthetic data with $m_1 = 100, m_2 = 250$ and rank $K = 5$. (Left) Objective value and consensus error of $\bar{\theta}_t^i$ against the DeFW iteration number t . Notice that the consensus error (in purple and yellow) / duality gap (in black) are plotted in a logarithmic scale (cf. the right y-axis) while the objective values are plotted in a linear scale; (Right) MSE against the DeFW iteration number t on the testing set.

rate predicted by Lemma 1. On the other hand, the top-right plot compares mean square error (MSE) of the predicted matrix θ for the testing set. Here, we also compare the result with the algorithm in [45]. We observe that the MSE performance of the DeFW algorithms approach their centralized counterpart as the iteration number grows, yet the algorithm in [45] achieves the best performance in this setting, notice that the true rank of θ_{true} is provided to this algorithm. From the bottom plot, the DPG method applied to square loss function converges at a relatively fast rate in the beginning, but was overtaken by DeFW as the iteration number grows. It is worth mentioning that the DeFW algorithms have a consistently better MSE performance than DPG.

The second example considers adding noise to the observations for the same synthetic data case in Fig. 1. In particular, we adopt the same setting as the previous example but include a *sparse* noise in the observations — here, each $Z_{k,l} = p_{k,l} \cdot \tilde{Z}_{k,l}$ where $p_{k,l}$ is Bernoulli with $P(p_{k,l} = 1) = 0.2$ and $\tilde{Z}_{k,l} \sim \mathcal{N}(0, 5)$ (cf. (32)). The convergence results are compared in Fig. 2. For the left plot, we observe similar convergence behaviors for the DeFW algorithms applied to different objective functions as in the previous example. On the right plot, we observe that the DeFW algorithm based on negated Gaussian loss achieves the lowest MSE, demonstrating its robustness to outlier noise. We also see that the algorithm in [45] performs poorly on this dataset.

Another interesting discovery is that the algorithm in [45] seems to fail when the rank of θ_{true} is high, even when the true rank is known and the observations are noiseless. In Fig. 3, we show the MSE against iteration number of the algorithms when the synthetic data is noiseless and generated with $m_1 = 100, m_2 = 250, K = 10$. As seen, [45] fails to produce a low MSE, while DeFW offers a reasonable performance.

The next example evaluates the objective value and test MSE on synthetic, noiseless data against the average runtime per agent. We focus on comparing the DeFW and DPG algorithms.

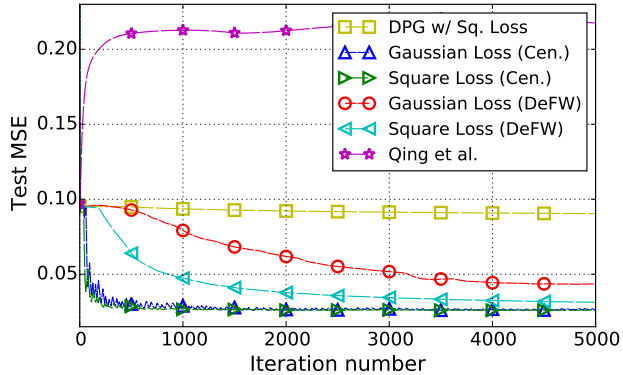


Figure 3: Convergence of test MSE against iteration number on the testing set on noise-free synthetic data with $m_1 = 100$, $m_2 = 250$ and rank $K = 10$.

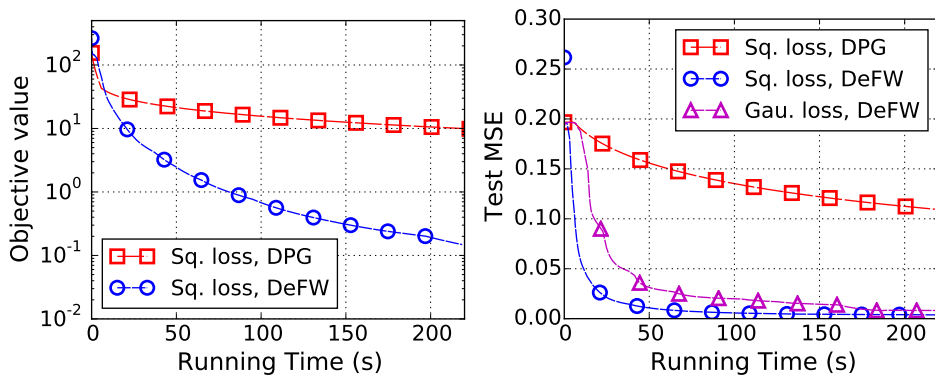


Figure 4: Results on noiseless synthetic data with $m_1 = 200$, $m_2 = 1000$ and rank $K = 5$. (Left) Objective value against running time. (Right) Worst-case MSE (among agents) against running time.

In Fig. 4, DeFW demonstrates a significant advantage over DPG since the former does not require the projection computation. In fact, the average running time *per iteration* of DeFW is five times faster than DPG. We also expect the complexity advantages to widen as the problem size grows.

Lastly, we consider the dataset `movielens100k`. We set $R = 10^5$ and focus on the test MSE evaluated against the iteration number for the proposed DeFW algorithm. The numerical results are presented in Fig. 5, where we also compare the case when we apply multiple ($\ell = 1, 3$) rounds of AC updates per iteration to speed up the algorithm. The left plot in Fig. 5 considers the noiseless scenario. As seen, the proposed DeFW algorithm applied on different loss functions converge to a reasonable MSE that is attained by the centralized FW algorithm. We see that the DeFW with negated Gaussian loss has a slower convergence compared to the square loss which is possibly attributed to the non-convexity of the loss function. Moreover, the algorithms achieve much faster convergence if we allow $\ell = 3$ AC rounds of network information exchange per iteration. The right plot in Fig. 5 considers when the observations are contaminated with a sparse noise of the same model as Fig. 2. We observe that the negated Gaussian loss implementations attain the best MSE as the non-convex loss is more robust against the sparse noise. Interestingly, the DeFW algorithm with $\ell = 3$ AC rounds has even outperformed its centralized counterpart. We suspect that this is caused by the DeFW algorithm converging to a different local minima for the non-convex problem.

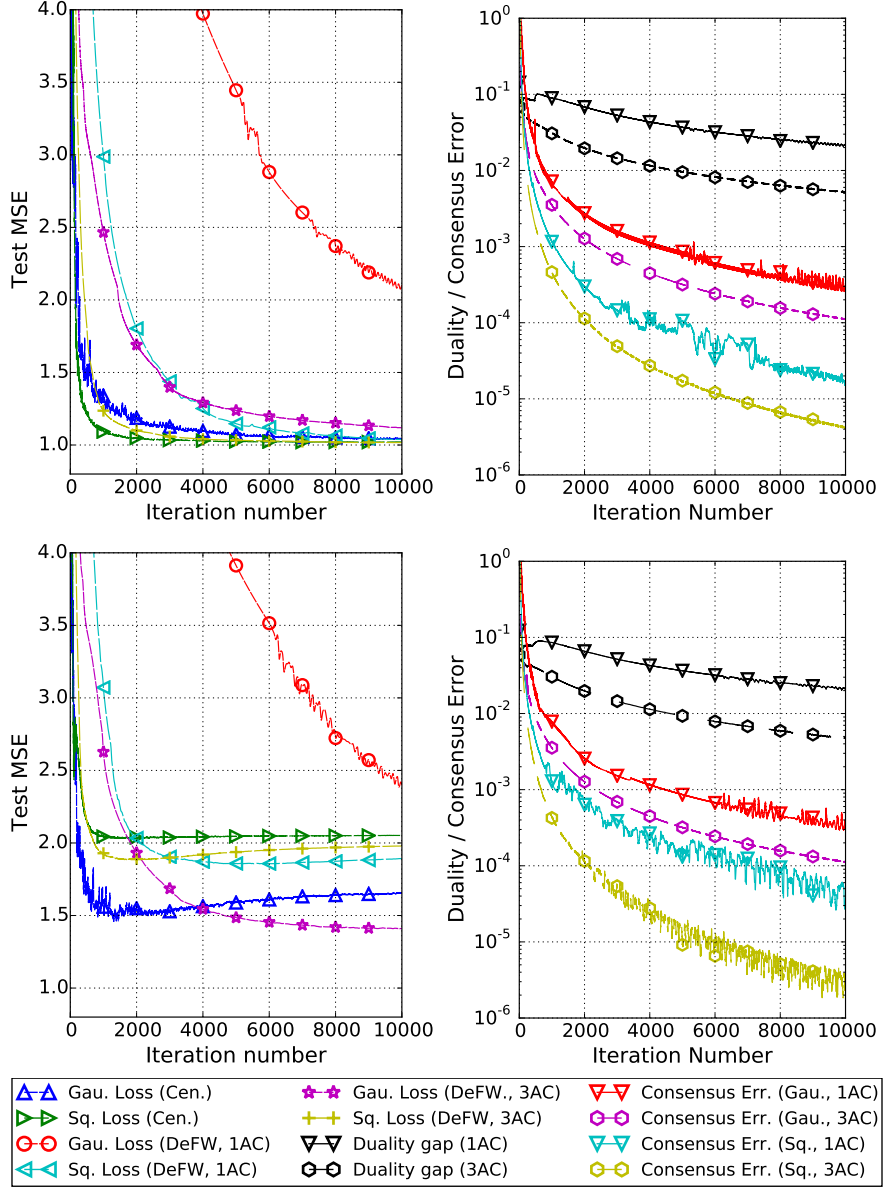


Figure 5: Convergence of the DeFW algorithm on `movielens100k`. (Top) Noiseless observations; (Bottom) sparse-noise contaminated observations. Note that the duality gap and consensus error are drawn in a logarithmic scale in the right plots.

5.2 Communication-efficient LASSO

This section conducts numerical experiments on the decentralized sparse learning problem. We focus on the *sparsified DeFW algorithm* in Section 4.2 that has better communication efficiency. We evaluate the performance on both synthetic and benchmark data. For the synthetic data, we randomly generate each \mathbf{A}_i as a $(m = 20) \times (d = 10000)$ matrix with $\mathcal{N}(0, 1)$ elements (cf. (37)) and $\boldsymbol{\theta}_{\text{true}}$ is a random sparse vector with $\|\boldsymbol{\theta}_{\text{true}}\|_0 = 50$ such that the non-zero elements are also $\mathcal{N}(0, 1)$. The observation noise \mathbf{z}_i has a variance of $\sigma^2 = 0.01$. For benchmark data, we test our method on

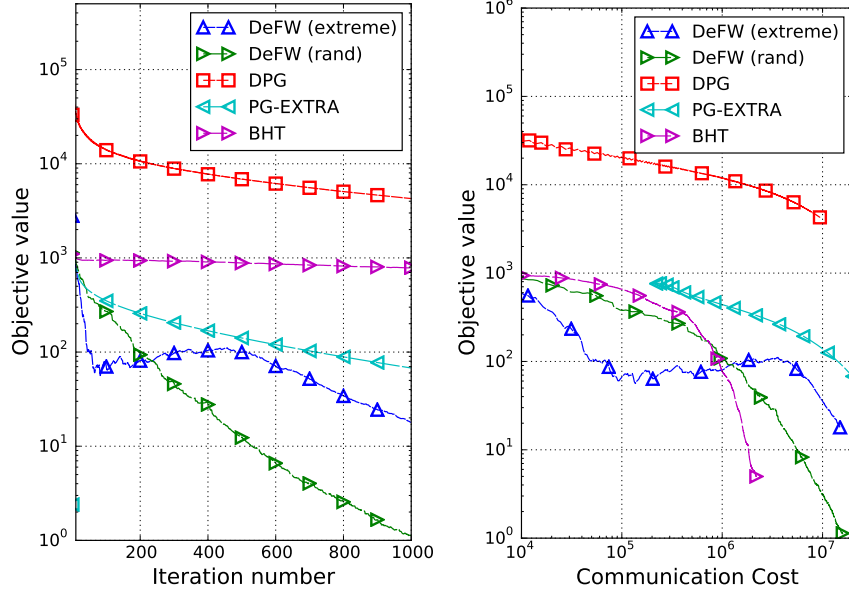


Figure 6: Convergence of the objective value on LASSO with synthetic dataset. (Left) against the iteration number. (Right) against the communication cost (i.e., total number of values transmitted/received in the network during AC updates). In the legend, ‘DeFW (extreme)’ refers to the extreme coordinate selection and ‘DeFW (rand)’ refers to the random coordinate selection scheme.

`sparco7` [57], which is a commonly used dataset for benchmarking sparse recovery algorithms. For `sparco7`, we have $\mathbf{A}_i \in \mathbb{R}^{12 \times 2560}$ as the local measurement matrix and $\boldsymbol{\theta}_{\text{true}}$ is a sparse vector with $\|\boldsymbol{\theta}_{\text{true}}\|_0 = 20$.

The sparsified DeFW algorithm is implemented with $p_t = \lceil 2 + \alpha_{\text{comm}} \cdot t \rceil$, $\ell_t = \lceil \log(t) + 1 \rceil$ with extreme or random coordinate selection. We compare the algorithms of PG-EXTRA [16] (with fixed step size $\alpha = 1/d$), DPG [15] (with step size $\alpha_t = 1/t$) and BHT [7]. DeFW, PG-EXTRA and DPG are set to solve the convex problem (38) with $R = 1.1\|\boldsymbol{\theta}_{\text{true}}\|_1$. BHT is a communication efficient decentralized version of IHT and is supplied with the true sparsity level in our simulations.

The first example in Fig. 6 shows the convergence of the algorithms on the synthetic data, where we compare the objective value against the number of iterations and the communication cost, i.e., total number of values sent during the distributed optimization. We set $\alpha_{\text{comm}} = 0.05$ for the DeFW algorithms. From the left plot, we observe that DeFW and PG-EXTRA algorithms have similar iteration complexity while ‘DeFW (rand)’ seems to have the fastest convergence. Meanwhile, BHT demands a high number of iterations for convergence. On the other hand, in the right plot, the DeFW algorithms demonstrate the best communication efficiency at low accuracy, while they lose to BHT at higher accuracy. Lastly, ‘DeFW (extreme)’ achieves a better accuracy at the beginning (i.e., less communication cost paid) but is overtaken by ‘DeFW (rand)’ as the communication cost grows.

We then compare the performance on `sparco7`, where we show the convergence of objective value against the communication cost in Fig. 7. We set $\alpha_{\text{comm}} = 0.025$ for the sparsified DeFW algorithms. At low accuracy, the DeFW algorithms offer the best communication cost-accuracy trade-off, i.e., it performs the best at an accuracy of above $\sim 10^{-2}$. Moreover, ‘DeFW (extreme)’ seems to be perform better than ‘DeFW (rand)’ in this example. Nevertheless, the BHT algorithm

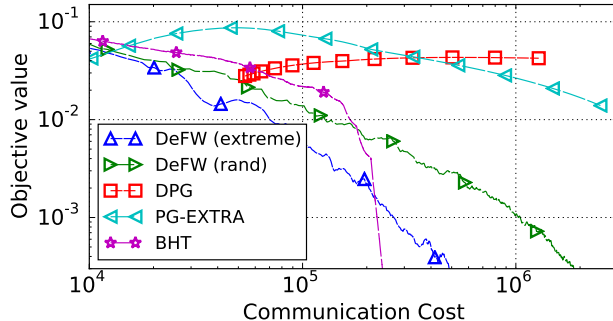


Figure 7: Convergence of the objective value against the communication cost on LASSO with `sparco7` dataset. In the legend, ‘DeFW (extreme)’ refers to the extreme coordinate selection and ‘DeFW (rand)’ refers to the random coordinate selection scheme.

achieves the best performance when the communication cost paid is above 3×10^5 . Lastly, we comment that although BHT has the lowest communication cost at *high* accuracy, its computational complexity is high as the former requires a large number of iterations to reach a reasonable accuracy (cf. left plot of Fig. 6). The sparsified DeFW offers a better balance of the communication and computation complexity.

6 Conclusions & Open Problems

In this paper, we have studied a decentralized projection-free algorithm for constrained optimization, which we called the DeFW algorithm. Importantly, we showed that the DeFW algorithm converges for both convex and non-convex loss functions and the respective convergence rates are analyzed. The efficacy of the proposed algorithm is demonstrated through tackling two problems related to machine learning, with the advantages over previous state-of-the-art demonstrated through numerical experiments. Future directions of study include developing an asynchronous version of the DeFW algorithm.

7 Acknowledgement

The authors would like to thank the anonymous reviewers for providing constructive comments on our paper.

A Proof of Theorem 1

The proof of Theorem 1 follows from our recent analysis on online/stochastic FW algorithm [39]. Using line 5 of Algorithm 1, we observe that:

$$\bar{\theta}_{t+1} = \bar{\theta}_t + \gamma_t (N^{-1} \sum_{i=1}^N \mathbf{a}_t^i - \bar{\theta}_t). \quad (45)$$

Define $h_t := F(\bar{\boldsymbol{\theta}}_t) - F(\boldsymbol{\theta}^*)$ where $\boldsymbol{\theta}^*$ is an optimal solution to (1). From the L -smoothness of F and the boundedness of \mathcal{C} , we have:

$$h_{t+1} \leq h_t + \frac{\gamma_t}{N} \sum_{i=1}^N \langle \mathbf{a}_t^i - \bar{\boldsymbol{\theta}}_t, \nabla F(\bar{\boldsymbol{\theta}}_t) \rangle + \gamma_t^2 \frac{L\bar{\rho}^2}{2}, \quad (46)$$

where $\bar{\rho}$ was defined in (5). Observe the following chain for the inner product: for each $i \in [N]$, we have

$$\begin{aligned} \langle \mathbf{a}_t^i - \bar{\boldsymbol{\theta}}_t, \nabla F(\bar{\boldsymbol{\theta}}_t) \rangle &\leq \langle \mathbf{a}_t^i - \bar{\boldsymbol{\theta}}_t, \overline{\nabla_t^i F} \rangle + \bar{\rho} \|\overline{\nabla_t^i F} - \nabla F(\bar{\boldsymbol{\theta}}_t)\|_2 \\ &\leq \langle \mathbf{a} - \bar{\boldsymbol{\theta}}_t, \overline{\nabla_t^i F} \rangle + \bar{\rho} \cdot \|\overline{\nabla_t^i F} - \nabla F(\bar{\boldsymbol{\theta}}_t)\|_2, \quad \forall \mathbf{a} \in \mathcal{C} \\ &\leq \langle \mathbf{a} - \bar{\boldsymbol{\theta}}_t, \nabla F(\bar{\boldsymbol{\theta}}_t) \rangle + 2\bar{\rho} \cdot \|\overline{\nabla_t^i F} - \nabla F(\bar{\boldsymbol{\theta}}_t)\|_2, \quad \forall \mathbf{a} \in \mathcal{C}, \end{aligned} \quad (47)$$

where we have added and subtracted $\overline{\nabla_t^i F}$ in the first inequality; and used the fact $\mathbf{a}_t^i \in \arg \min_{\mathbf{a} \in \mathcal{C}} \langle \mathbf{a}, \overline{\nabla_t^i F} \rangle$ in the second inequality. Recalling that $\overline{\nabla_t F} = N^{-1} \sum_{i=1}^N \overline{\nabla_t^i F}$,

$$\begin{aligned} \|\overline{\nabla_t F} - \nabla F(\bar{\boldsymbol{\theta}}_t)\|_2 &\leq \|\overline{\nabla_t^i F} - \overline{\nabla_t F}\|_2 + \|\overline{\nabla_t F} - \nabla F(\bar{\boldsymbol{\theta}}_t)\|_2 \\ &\leq \Delta d_t + N^{-1} \sum_{i=1}^N \|\nabla f_i(\bar{\boldsymbol{\theta}}_t^i) - \nabla f_i(\bar{\boldsymbol{\theta}}_t)\|_2 \\ &\leq \Delta d_t + L \cdot N^{-1} \sum_{i=1}^N \|\bar{\boldsymbol{\theta}}_t^i - \bar{\boldsymbol{\theta}}_t\|_2 \\ &\leq \Delta d_t + L \cdot \Delta p_t, \end{aligned} \quad (48)$$

where the third inequality is due to the L -smoothness of $\{f_i\}_{i=1}^N$. Recalling that $\Delta p_t = C_p/t$, $\Delta d_t = C_g/t$ and substituting the results above into the inequality (46) implies:

$$h_{t+1} \leq h_t + \gamma_t \langle \bar{\mathbf{a}}_t - \bar{\boldsymbol{\theta}}_t, \nabla F(\bar{\boldsymbol{\theta}}_t) \rangle + \gamma_t^2 \frac{L\bar{\rho}^2}{2} + 2\bar{\rho}\gamma_t \frac{C_g + LC_p}{t}, \quad (49)$$

where $\bar{\mathbf{a}}_t \in \mathcal{C}$ is the minimizer of the linear optimization (7a) using $\nabla F(\bar{\boldsymbol{\theta}}_t)$, i.e.,

$$\bar{\mathbf{a}}_t \in \arg \min_{\mathbf{a} \in \mathcal{C}} \langle \mathbf{a}, \nabla F(\bar{\boldsymbol{\theta}}_t) \rangle. \quad (50)$$

Case 1: When F is convex, we observe

$$\langle \bar{\mathbf{a}}_t - \bar{\boldsymbol{\theta}}_t, \nabla F(\bar{\boldsymbol{\theta}}_t) \rangle \leq \langle \boldsymbol{\theta}^* - \bar{\boldsymbol{\theta}}_t, \nabla F(\bar{\boldsymbol{\theta}}_t) \rangle \leq -h_t, \quad (51)$$

where the first inequality is due to the optimality of $\bar{\mathbf{a}}_t$ and the last inequality stems from the convexity of F . Plugging the above into (49) yields

$$h_{t+1} \leq (1 - \gamma_t)h_t + \gamma_t^2 \frac{L\bar{\rho}^2}{2} + \gamma_t \frac{2\bar{\rho}(C_g + LC_p)}{t}. \quad (52)$$

As $\gamma_t = 2/(t+1)$, from a high-level point of view, the above inequality behaves similarly to $h_{t+1} \leq (1 - (1/t))h_t + \mathcal{O}(1/t^2)$. Consequently, applying [58, Lemma 4] yields a $\mathcal{O}(1/t)$ convergence rate for h_t . In fact, this is a deterministic version of the case analyzed by [39, Theorem 10]. In particular, setting $\alpha = 1, K = 2$ in [39, (56)] and using an induction argument yield

$$h_t \leq 2 \cdot (4\bar{\rho}(C_g + LC_p) + L\bar{\rho}^2)/(t+1), \quad \forall t \geq 1. \quad (53)$$

Case 2: For the case when F is μ -strongly convex and θ^* lies in the interior of \mathcal{C} with distance $\delta > 0$ (cf. (6)). Using [39, Lemma 6], we have

$$\langle \bar{\theta}_t - \bar{\mathbf{a}}_t, \nabla F(\bar{\theta}_t) \rangle \geq \sqrt{2\mu\delta^2 h_t}. \quad (54)$$

Plugging the above into (49) gives

$$h_{t+1} \leq \sqrt{h_t}(\sqrt{h_t} - \gamma_t \sqrt{2\mu\delta^2}) + \gamma_t^2 \frac{L\bar{\rho}^2}{2} + \gamma_t \frac{2\bar{\rho}(C_g + LC_p)}{t}. \quad (55)$$

Compared to the case analyzed in (52), when h_t is decreased, the decrement in h_{t+1} is increased, leading to a faster convergence. This is a deterministic version of the case analyzed in [39, Theorem 7]. Setting $\alpha = 1, K = 2$ in [39, (48)] and using an induction argument yields

$$h_t \leq \frac{(4\bar{\rho}(C_g + LC_p) + L\bar{\rho}^2)^2}{2\delta^2\mu} \cdot \frac{9}{(t+1)^2}, \quad \forall t \geq 1. \quad (56)$$

B Proof of Theorem 2

B.1 Convergence rate

Let us recall the definition of the *FW gap*:

$$g_t := \max_{\theta \in \mathcal{C}} \langle \nabla F(\bar{\theta}_t), \bar{\theta}_t - \theta \rangle = \langle \nabla F(\bar{\theta}_t), \bar{\theta}_t - \bar{\mathbf{a}}_t \rangle, \quad (57)$$

where we have used the definition of $\bar{\mathbf{a}}_t$ in (50) from the previous proof. For simplicity, we shall assume that T is an even integer in the following.

From the L -smoothness of F , we have:

$$F(\bar{\theta}_{t+1}) \leq F(\bar{\theta}_t) + \langle \nabla F(\bar{\theta}_t), \bar{\theta}_{t+1} - \bar{\theta}_t \rangle + \frac{L}{2} \|\bar{\theta}_{t+1} - \bar{\theta}_t\|_2^2. \quad (58)$$

Observe that:

$$\bar{\theta}_{t+1} - \bar{\theta}_t = N^{-1} \sum_{i=1}^N \gamma_t (\mathbf{a}_i^t - \bar{\theta}_t^i). \quad (59)$$

As $\mathbf{a}_i^t, \bar{\theta}_t^i \in \mathcal{C}$, we have $\|\bar{\theta}_{t+1} - \bar{\theta}_t\|_2 \leq \gamma_t \bar{\rho}$. Using (47) and (48) from the previous proof of Theorem 1, the inequality (58) can be bounded as:

$$\begin{aligned} F(\bar{\theta}_{t+1}) &\leq F(\bar{\theta}_t) - \gamma_t \langle \nabla F(\bar{\theta}_t), \bar{\theta}_t - \bar{\mathbf{a}}_t \rangle \\ &\quad + 2\gamma_t \bar{\rho} \cdot (\Delta d_t + L \cdot \Delta p_t) + \gamma_t^2 L \bar{\rho}^2 / 2 \\ &= F(\bar{\theta}_t) - \gamma_t g_t + 2\gamma_t \bar{\rho} \cdot (\Delta d_t + L \cdot \Delta p_t) + \gamma_t^2 \frac{L \bar{\rho}^2}{2}. \end{aligned} \quad (60)$$

From the definition, we observe that $g_t \geq 0$. Now, summing the two sides of (60) from $t = T/2 + 1$ to $t = T$ gives:

$$\begin{aligned} \sum_{t=T/2+1}^T \gamma_t g_t &\leq \sum_{t=T/2+1}^T \left(F(\bar{\theta}_t) - F(\bar{\theta}_{t+1}) \right) \\ &\quad + \sum_{t=T/2+1}^T \left(2\gamma_t \bar{\rho} \cdot (\Delta d_t + L \cdot \Delta p_t) + \gamma_t^2 \frac{L \bar{\rho}^2}{2} \right). \end{aligned} \quad (61)$$

Canceling duplicated terms in the first term of the right hand side above gives:

$$\begin{aligned} \sum_{t=T/2+1}^T \gamma_t g_t &\leq F(\bar{\boldsymbol{\theta}}_{T/2+1}) - F(\bar{\boldsymbol{\theta}}_{T+1}) \\ &+ \sum_{t=T/2+1}^T \left(2\gamma_t \bar{\rho} \cdot (\Delta d_t + L \cdot \Delta p_t) + \gamma_t^2 \frac{L\bar{\rho}^2}{2} \right). \end{aligned} \quad (62)$$

As $g_t, \gamma_t \geq 0$, we can lower bound the left hand side as:

$$\sum_{t=T/2+1}^T \gamma_t g_t \geq \left(\min_{t \in [T/2+1, T]} g_t \right) \cdot \left(\sum_{t=T/2+1}^T \gamma_t \right), \quad (63)$$

and observe that for all $T \geq 6$ and $\alpha \in (0, 1)$,

$$\sum_{t=T/2+1}^T \gamma_t \geq \frac{T^{1-\alpha}}{1-\alpha} \cdot \left(1 - \left(\frac{2}{3} \right)^{1-\alpha} \right) = \Omega(T^{1-\alpha}). \quad (64)$$

Define the constant $C := L\bar{\rho}^2/2 + 2\bar{\rho}(C_g + LC_p)$. When $\alpha \geq 0.5$, using the fact that $\gamma_t = t^{-\alpha}$, $\Delta p_t = C_p/t^\alpha$, $\Delta d_t = C_g/t^\alpha$, the right hand side of (62) is bounded above by:

$$G \cdot \rho + C \cdot \sum_{t=T/2+1}^T t^{-2\alpha} \leq G \cdot \rho + C \cdot \log 2, \quad (65)$$

note that the series is converging as we are summing from $t = T/2 + 1$ to $t = T$. Dividing the above term by the lower bound (64) to $\sum_{t=T/2+1}^T \gamma_t$ yields (16).

On the other hand, when $\alpha < 0.5$, we notice that

$$\sum_{t=T/2+1}^T t^{-2\alpha} \leq \int_{T/2}^T t^{-2\alpha} dt = \frac{2^{1-2\alpha} - 1}{1 - 2\alpha} \left(\frac{T}{2} \right)^{1-2\alpha}. \quad (66)$$

Therefore, the right hand side of (62) is bounded above by

$$G\rho + C \sum_{t=T/2+1}^T t^{-2\alpha} \leq \left(G\rho + C \frac{1 - (1/2)^{1-2\alpha}}{1 - 2\alpha} \right) \cdot T^{1-2\alpha}. \quad (67)$$

Dividing the above term by the lower bound (64) to $\sum_{t=T/2+1}^T \gamma_t$ yields (17).

B.2 Convergence to stationary point of (1)

Recall that the set of stationary points to (1) is defined as:

$$\mathcal{C}^* := \{ \bar{\boldsymbol{\theta}} \in \mathcal{C} : \max_{\boldsymbol{\theta} \in \mathcal{C}} \langle \nabla F(\bar{\boldsymbol{\theta}}), \bar{\boldsymbol{\theta}} - \boldsymbol{\theta} \rangle = 0 \}. \quad (68)$$

We state the following Nurminskii's sufficient condition:

Theorem 3 [59, Theorem 1] Consider a sequence $\{\bar{\theta}_t\}_{t \geq 1}$ in a compact set \mathcal{C} . Suppose that the following hold⁵:

A.1 $\lim_{t \rightarrow \infty} \|\bar{\theta}_{t+1} - \bar{\theta}_t\| = 0$.

A.2 Let $\underline{\theta}$ be a limit point of $\{\bar{\theta}_t\}_{t \geq 1}$ and $\{\theta_{s_t}\}_{t \geq 1}$ be a subsequence that converges to $\underline{\theta}$. If $\underline{\theta} \notin \mathcal{C}^*$, then for any t and some sufficiently small $\epsilon > 0$, there exists a finite s such that $\|\bar{\theta}_s - \bar{\theta}_{s_t}\| > \epsilon$ and $s > s_t$.

A.3 Let $\underline{\theta}$ be a limit point of $\{\bar{\theta}_t\}_{t \geq 1}$ and $\{\theta_{s_t}\}_{t \geq 1}$ be a subsequence that converges to $\underline{\theta}$. If $\underline{\theta} \notin \mathcal{C}^*$, then for any t and some sufficiently small $\epsilon > 0$, we can define

$$\tau_t := \min_{s > s_t} s \quad \text{s.t.} \quad \|\bar{\theta}_s - \bar{\theta}_{s_t}\| > \epsilon \quad (69)$$

where τ_t is finite. Also, there exists a continuous function $W(\bar{\theta})$ that takes a finite number of values in \mathcal{C}^* with

$$\limsup_{t \rightarrow \infty} W(\bar{\theta}_{\tau_t}) < \lim_{t \rightarrow \infty} W(\bar{\theta}_{s_t}). \quad (70)$$

Then the sequence $\{W(\bar{\theta}_t)\}_{t \geq 1}$ converges and the limit points of the sequence $\{\bar{\theta}_t\}_{t \geq 1}$ belongs to the set \mathcal{C}^* .

We apply the above theorem to prove that every limit point of $\{\bar{\theta}_t\}_{t \geq 1}$ are in \mathcal{C}^* . First, A.1 can be easily verified since

$$\|\bar{\theta}_{t+1} - \bar{\theta}_t\| \leq \frac{\gamma_t}{N} \sum_{i=1}^N \|\mathbf{a}_t^i - \bar{\theta}_t\| \leq \frac{\gamma_t \bar{\rho}}{N} \quad (71)$$

and we have $\gamma_t \rightarrow 0$ as $t \rightarrow \infty$.

As \mathcal{C} is compact, there exists a convergent subsequence $\{\bar{\theta}_{s_t}\}_{t \geq 1}$ of the sequence of iterates generated by the DeFW algorithm. Let $\underline{\theta}$ be the limit point of $\{\bar{\theta}_{s_t}\}_{t \geq 1}$ and $\underline{\theta} \notin \mathcal{C}^*$. We shall verify A.2 by contradiction. In particular, fix a sufficiently small $\epsilon > 0$ and assume that the following holds:

$$\|\bar{\theta}_s - \bar{\theta}_{s_t}\| \leq \epsilon, \quad \forall s > s_t, \quad \forall t \geq 1. \quad (72)$$

As $\{\bar{\theta}_{s_t}\}_{t \geq 1}$ converges to $\underline{\theta}$, the assumption (72) implies that for some sufficiently large t and any $s > s_t$, we have $\bar{\theta}_s \in \mathcal{B}_{2\epsilon}(\underline{\theta})$, i.e., the ball of radius 2ϵ centered at $\underline{\theta}$.

Since $\underline{\theta} \notin \mathcal{C}^*$, the following holds for some $\delta > 0$,

$$\langle \nabla F(\bar{\theta}_s), \underline{\theta} - \bar{\theta}_s \rangle \leq -\delta < 0, \quad \forall \underline{\theta} \in \mathcal{C}, \quad \forall s > s_t. \quad (73)$$

In particular, we have $\langle \nabla F(\bar{\theta}_s), \bar{\mathbf{a}}_s - \bar{\theta}_s \rangle \leq -\delta$ as we recall that $\bar{\mathbf{a}}_s = \arg \min_{\mathbf{a} \in \mathcal{C}} \langle \nabla F(\bar{\theta}_s), \mathbf{a} \rangle$.

On the other hand, from (60) and using Assumptions 1-2, it holds true for all $t \geq 1$ that:

$$\begin{aligned} F(\bar{\theta}_{t+1}) - F(\bar{\theta}_t) &\leq \gamma_t \cdot \langle \nabla F(\bar{\theta}_t), \bar{\mathbf{a}}_t - \bar{\theta}_t \rangle \\ &\quad + \gamma_t \cdot \mathcal{O}(t^{-\alpha}) + \gamma_t^2 L \bar{\rho}^2 / 2. \end{aligned} \quad (74)$$

⁵To give a clearer presentation, we have rephrased conditions A.2 and A.3 from the original Nurminkii's conditions.

To arrive at a contradiction, we let $s > s_t$ and sum up the two sides of (74) from $t = s_t$ to $t = s$. Consider the following chain of inequality:

$$\begin{aligned} F(\bar{\boldsymbol{\theta}}_s) - F(\bar{\boldsymbol{\theta}}_{s_t}) &\leq \sum_{\ell=s_t}^s \gamma_\ell (\nabla F(\bar{\boldsymbol{\theta}}_\ell), \bar{\mathbf{a}}_\ell - \bar{\boldsymbol{\theta}}_\ell) + \mathcal{O}(\ell^{-\alpha}) \\ &\leq -\delta \sum_{\ell=s_t}^s \gamma_\ell + \sum_{\ell=s_t}^s \gamma_\ell \mathcal{O}(\ell^{-\alpha}), \end{aligned} \quad (75)$$

where the first inequality is due to the fact that $\gamma_\ell^2 L \bar{\rho}^2 / 2 = \gamma_\ell \mathcal{O}(\ell^{-\alpha})$ and the second inequality is due to (73). Rearranging terms in (75), we have

$$F(\bar{\boldsymbol{\theta}}_s) - F(\bar{\boldsymbol{\theta}}_{s_t}) - \sum_{\ell=s_t}^s C \cdot \ell^{-2\alpha} \leq -\delta \sum_{\ell=s_t}^s \ell^{-\alpha}, \quad (76)$$

for some $C < \infty$. As $1 \geq \alpha > 0.5$, we have $\lim_{s \rightarrow \infty} \sum_{\ell=s_t}^s \ell^{-2\alpha} < \infty$ on the left hand side and $\lim_{s \rightarrow \infty} \sum_{\ell=s_t}^s \ell^{-\alpha} \rightarrow +\infty$ on the right hand side. Letting $s \rightarrow \infty$ on the both side of (76) implies

$$\lim_{s \rightarrow \infty} F(\bar{\boldsymbol{\theta}}_s) - F(\bar{\boldsymbol{\theta}}_{s_t}) < -\infty, \quad (77)$$

This leads to a contradiction to (73) since $F(\boldsymbol{\theta})$ is bounded over \mathcal{C} . We conclude that A.2 holds for the DeFW algorithm.

The remaining task is to verify A.3. We notice that the indices τ_t in (69) are well defined since A.2 holds. Take $W(\boldsymbol{\theta}) = F(\boldsymbol{\theta})$ and notice that the image $F(\mathcal{C}^*)$ is a finite set (cf. Assumption 3). By the definition of τ_t , we have $\bar{\boldsymbol{\theta}}_s \in \mathcal{B}_\epsilon(\bar{\boldsymbol{\theta}}_{s_t})$ for all $s_t \leq s \leq \tau_t - 1$. Again for some sufficiently large t , we have $\bar{\boldsymbol{\theta}}_s \in \mathcal{B}_\epsilon(\bar{\boldsymbol{\theta}}_{s_t}) \subseteq \mathcal{B}_{2\epsilon}(\bar{\boldsymbol{\theta}})$ and the inequality (75) holds for $s = \tau_t - 1$. This gives:

$$F(\bar{\boldsymbol{\theta}}_{\tau_t}) - F(\bar{\boldsymbol{\theta}}_{s_t}) \leq \sum_{\ell=s_t}^{\tau_t-1} \gamma_\ell \cdot (-\delta + \mathcal{O}(\ell^{-\alpha})). \quad (78)$$

On the other hand, we have $\bar{\boldsymbol{\theta}}_{\tau_t} \notin \mathcal{B}_\epsilon(\bar{\boldsymbol{\theta}}_{s_t})$ and thus

$$\epsilon < \|\bar{\boldsymbol{\theta}}_{\tau_t} - \bar{\boldsymbol{\theta}}_{s_t}\| \leq \sum_{\ell=s_t}^{\tau_t-1} \gamma_\ell \left\| \sum_{i=1}^N \frac{\mathbf{a}_\ell^i}{N} - \bar{\boldsymbol{\theta}}_\ell \right\| \leq \bar{\rho} \sum_{\ell=s_t}^{\tau_t-1} \gamma_\ell. \quad (79)$$

The above implies that $\sum_{\ell=s_t}^{\tau_t-1} \gamma_\ell > \epsilon / \bar{\rho} > 0$. Considering (78) again, observe that $\mathcal{O}(\ell^{-\alpha})$ decays to zero, for some sufficiently large t , we have $-\delta + \mathcal{O}(\ell^{-\alpha}) \leq -\delta' < 0$ if $\ell \geq s_t$. Therefore, (78) leads to

$$F(\bar{\boldsymbol{\theta}}_{\tau_t}) - F(\bar{\boldsymbol{\theta}}_{s_t}) \leq -\delta' \sum_{\ell=s_t}^{\tau_t-1} \gamma_\ell < -\frac{\delta' \epsilon}{\bar{\rho}} < 0. \quad (80)$$

Taking the limit $t \rightarrow \infty$ on both sides leads to (70). The proof for the convergence to stationary point in Theorem 2 is completed by applying Theorem 3.

C Proof of Lemma 1

For simplicity, we shall drop the dependence of α in the constant $t_0(\alpha)$. It suffices to show that for all $t \geq 1$,

$$\sqrt{\sum_{i=1}^N \|\bar{\boldsymbol{\theta}}_t^i - \bar{\boldsymbol{\theta}}_t\|_2^2} \leq \frac{C_p}{t^\alpha}, \quad C_p = (t_0)^\alpha \cdot \sqrt{N} \bar{\rho}. \quad (81)$$

We observe that for $t = 1$ to $t = t_0$, the above inequality is true since $\bar{\boldsymbol{\theta}}_t^i, \bar{\boldsymbol{\theta}}_t \in \mathcal{C}$ and the diameter of \mathcal{C} is bounded by $\bar{\rho}$. For the induction step, let us assume that $\sqrt{\sum_{i=1}^N \|\bar{\boldsymbol{\theta}}_t^i - \bar{\boldsymbol{\theta}}_t\|_2^2} \leq C_p/t^\alpha$ for some $t \geq t_0$. Observe that

$$\boldsymbol{\theta}_{t+1}^i = (1 - t^{-\alpha})\bar{\boldsymbol{\theta}}_t^i + t^{-\alpha}\mathbf{a}_t^i. \quad (82)$$

Denote $\tilde{\mathbf{a}}_t = N^{-1} \sum_{i=1}^N \mathbf{a}_t^i$ and using Fact 1, we observe that,

$$\begin{aligned} \sum_{i=1}^N \|\bar{\boldsymbol{\theta}}_{t+1}^i - \bar{\boldsymbol{\theta}}_{t+1}\|_2^2 &\leq \\ &|\lambda_2(\mathbf{W})|^2 \cdot \sum_{j=1}^N \|(1 - t^{-\alpha})(\bar{\boldsymbol{\theta}}_t^j - \bar{\boldsymbol{\theta}}_t) + t^{-\alpha}(\mathbf{a}_t^j - \tilde{\mathbf{a}}_t)\|_2^2, \end{aligned} \quad (83)$$

where we have used the fact $\bar{\boldsymbol{\theta}}_{t+1} = (1 - t^{-\alpha})\bar{\boldsymbol{\theta}}_t + t^{-\alpha}\tilde{\mathbf{a}}_t$. The right hand side in the above can be bounded by

$$\begin{aligned} &\sum_{j=1}^N \|(1 - t^{-\alpha})(\bar{\boldsymbol{\theta}}_t^j - \bar{\boldsymbol{\theta}}_t) + t^{-\alpha}(\mathbf{a}_t^j - \tilde{\mathbf{a}}_t)\|_2^2 \\ &\leq \sum_{j=1}^N (\|\bar{\boldsymbol{\theta}}_t^j - \bar{\boldsymbol{\theta}}_t\|_2^2 + t^{-2\alpha}\bar{\rho}^2 + 2\bar{\rho}t^{-\alpha}\|\bar{\boldsymbol{\theta}}_t^j - \bar{\boldsymbol{\theta}}_t\|_2) \\ &\leq t^{-2\alpha}(C_p^2 + N\bar{\rho}^2) + 2\bar{\rho}t^{-\alpha}\sqrt{N} \sqrt{\sum_{j=1}^N \|\bar{\boldsymbol{\theta}}_t^j - \bar{\boldsymbol{\theta}}_t\|_2^2} \\ &\leq t^{-2\alpha}(C_p + \sqrt{N}\bar{\rho})^2 \leq \left(\frac{(t_0)^\alpha + 1}{(t_0)^\alpha \cdot t^\alpha} \cdot C_p\right)^2, \end{aligned} \quad (84)$$

where we have used the boundedness of \mathcal{C} in the first inequality, the norm equivalence $\sum_{j=1}^N |c_j| \leq \sqrt{N} \sqrt{\sum_{j=1}^N c_j^2}$ in the second inequality and the induction hypothesis in the third and fourth inequalities. Consequently, from (23), we observe that for all $t \geq t_0$,

$$|\lambda_2(\mathbf{W})| \cdot \frac{(t_0)^\alpha + 1}{(t_0)^\alpha \cdot t^\alpha} \leq \frac{1}{(t+1)^\alpha}, \quad (85)$$

and the induction step is completed. Finally, Lemma 1 is proven by observing that (81) implies (25).

D Proof of Lemma 2

We prove the first condition (29) with a simple induction. This condition is obviously true for the base step $t = 1$. For induction step, suppose that (29) is true up to some t , then

$$\sum_{i=1}^N \nabla_{t+1}^i F = \sum_{i=1}^N (\overline{\nabla_t^i F} - \nabla f_i(\bar{\boldsymbol{\theta}}_t^i)) + \sum_{i=1}^N \nabla f_i(\bar{\boldsymbol{\theta}}_{t+1}^i). \quad (86)$$

Note that the first term on the right hand side is zero due to the induction hypothesis. Thus, the induction step is completed and $N^{-1} \sum_{i=1}^N \nabla_t^i F = N^{-1} \sum_{i=1}^N \nabla f_i(\bar{\boldsymbol{\theta}}_t^i)$ for all $t \geq 1$.

Then, we prove the second condition (30). For simplicity, we drop the dependence of α in the constant $t_0(\alpha)$. Recall $\overline{\nabla_t F} := N^{-1} \sum_{i=1}^N \overline{\nabla_t^i F}$. It suffices to prove:

$$\sqrt{\sum_{i=1}^N \|\overline{\nabla_t^i F} - \overline{\nabla_t F}\|_2^2} \leq \frac{C_g}{t^\alpha}, \quad C_g = 2\sqrt{N}(t_0)^\alpha(2C_p + \bar{\rho})L \quad (87)$$

for all $t \geq 1$ using induction. For $t = 1$ to $t = t_0$, the inequality can be easily proven using the boundedness of the gradients. For the induction step, we suppose that $\sqrt{\sum_{i=1}^N \|\overline{\nabla_t^i F} - \overline{\nabla_t F}\|_2^2} \leq C_g/t^\alpha$ for some $t \geq t_0$. Define the slack variable $\delta f_{t+1}^i := \nabla f_i(\bar{\boldsymbol{\theta}}_{t+1}^i) - \nabla f_i(\bar{\boldsymbol{\theta}}_t^i)$. We observe that $\nabla_{t+1}^i F = \delta f_{t+1}^i + \overline{\nabla_t^i F}$ and $\overline{\nabla_{t+1}^i F} = \sum_{j=1}^N W_{ij} \nabla_{t+1}^j F$, thus applying Fact 1 yields

$$\begin{aligned} \sum_{i=1}^N \|\overline{\nabla_{t+1}^i F} - \overline{\nabla_{t+1} F}\|_2^2 &\leq \\ &|\lambda_2(\mathbf{W})|^2 \cdot \sum_{i=1}^N \|\overline{\nabla_t^i F} + \delta f_{t+1}^i - \overline{\nabla_{t+1} F}\|_2^2, \end{aligned} \quad (88)$$

Similarly, define $\delta F_{t+1} := \overline{\nabla_{t+1} F} - \overline{\nabla_t F} = N^{-1} \sum_{i=1}^N \delta f_{t+1}^i$ and observe that we can bound the right hand side of (88) as

$$\begin{aligned} &\sum_{i=1}^N \|\overline{\nabla_t^i F} + \delta f_{t+1}^i - \overline{\nabla_{t+1} F}\|_2^2 \\ &\leq \sum_{i=1}^N \left(\|\overline{\nabla_t^i F} - \overline{\nabla_t F}\|_2^2 + \|\delta f_{t+1}^i - \delta F_{t+1}\|_2^2 \right. \\ &\quad \left. + 2 \cdot \|\delta f_{t+1}^i - \delta F_{t+1}\|_2 \cdot \|\overline{\nabla_t^i F} - \overline{\nabla_t F}\|_2 \right) \end{aligned} \quad (89)$$

where the first inequality is obtained by expanding the squared ℓ_2 norm and applying Cauchy-Schwartz inequality.

Observe that for all $i \in [N]$, we have the following chain:

$$\begin{aligned} \|\delta f_{t+1}^i\|_2 &= \|\nabla f_i(\bar{\boldsymbol{\theta}}_{t+1}^i) - \nabla f_i(\bar{\boldsymbol{\theta}}_t^i)\|_2 \leq L \|\bar{\boldsymbol{\theta}}_{t+1}^i - \bar{\boldsymbol{\theta}}_t^i\|_2 \\ &\leq L \left\| \sum_{j=1}^N W_{ij} ((\boldsymbol{\theta}_{t+1}^j - \bar{\boldsymbol{\theta}}_t^j) + (\bar{\boldsymbol{\theta}}_t^j - \bar{\boldsymbol{\theta}}_t^i)) \right\|_2 \\ &\leq L \sum_{j=1}^N W_{ij} \left(t^{-\alpha} \bar{\rho} + 2C_p t^{-\alpha} \right) = (2C_p + \bar{\rho}) L t^{-\alpha}, \end{aligned} \quad (90)$$

where the last inequality is due to the convexity of ℓ_2 norm, the update rule in line 5 of Algorithm 1 and the results from Lemma 1. Using the triangular inequality, we observe that

$$\begin{aligned} \|\delta f_{t+1}^i - \delta F_{t+1}\|_2 &= \left\| \left(1 - \frac{1}{N}\right) \delta_{t+1}^i + \frac{1}{N} \sum_{j \neq i} \delta_{t+1}^j \right\|_2 \\ &\leq \left(1 - \frac{1}{N}\right) \|\delta_{t+1}^i\|_2 + \frac{1}{N} \sum_{j \neq i} \|\delta_{t+1}^j\|_2 \\ &\leq 2\left(1 - \frac{1}{N}\right) (2C_p + \bar{\rho}) L t^{-\alpha} \leq 2(2C_p + \bar{\rho}) L t^{-\alpha}. \end{aligned} \quad (91)$$

Finally, applying the induction hypothesis, the right hand side of Eq. (89) can be bounded by

$$\begin{aligned} &\sum_{i=1}^N \|\overline{\nabla_t^i F} + \delta f_{t+1}^i - \overline{\nabla_{t+1} F}\|_2^2 \\ &\leq t^{-2\alpha} (C_g^2 + 4N(2C_p + \bar{\rho})^2 L^2) \\ &\quad + t^{-\alpha} 4L(2C_p + \bar{\rho}) \sqrt{N} \sqrt{\sum_{i=1}^N \|\overline{\nabla_t^i F} - \overline{\nabla_t F}\|_2^2} \\ &\leq t^{-2\alpha} \cdot (C_g + 2L\sqrt{N}(2C_p + \bar{\rho}))^2 \leq \left(\frac{(t_0)^\alpha + 1}{(t_0)^\alpha \cdot t^\alpha} \cdot C_g\right)^2, \end{aligned}$$

where we have used the fact that $\sum_{i=1}^N \|\overline{\nabla_t^i F} - \overline{\nabla_t F}\|_2 \leq \sqrt{N} \sqrt{\sum_{i=1}^N \|\overline{\nabla_t^i F} - \overline{\nabla_t F}\|_2^2}$ in the first inequality. Invoking (23), we can upper bound the right hand side of (88) by $C_g^2/(t+1)^{2\alpha}$ for all $t \geq t_0$. Taking square root on both sides of the inequality completes the induction step. Consequently, (30) can be implied by (87).

E Proof of Lemma 3

Applying triangular inequality on the error vector yields:

$$\begin{aligned} &\left\| \xi_t^{-1} \overline{\nabla_t^i F} - \frac{1}{N} \sum_{j=1}^N \nabla f_j(\bar{\theta}_t^j) \right\|_\infty \\ &\leq \xi_t^{-1} \cdot \left\| \overline{\nabla_t^i F} - \frac{1}{N} \sum_{j=1}^N \nabla f_j(\bar{\theta}_t^j) \odot \mathbf{1}_{\Omega_t} \right\|_\infty \\ &\quad + \left\| \left(\frac{1}{N} \sum_{j=1}^N \nabla f_j(\bar{\theta}_t^j) \right) \odot (\xi_t^{-1} \mathbf{1}_{\Omega_t} - \mathbf{1}) \right\|_\infty, \end{aligned} \quad (92)$$

where $\mathbf{1}$ denotes the all-one vector. For the first term in the right hand side of (92), observe that $\overline{\nabla_t^i F}$ is obtained by applying the AC updates on the sparsified local gradients $\nabla f_i(\bar{\theta}_t^i) \odot \mathbf{1}_{\Omega_t}$ for $\ell_t = \lceil C_l + \log(t)/\log|\lambda_2^{-1}(\mathbf{W})| \rceil$ rounds, applying Fact 1 yields the following for all $i \in [N]$:

$$\begin{aligned} &\left\| \overline{\nabla_t^i F} - \frac{1}{N} \sum_{j=1}^N \nabla f_j(\bar{\theta}_t^j) \odot \mathbf{1}_{\Omega_t} \right\|_\infty \\ &\leq |\lambda_2(\mathbf{W})|^{\ell_t} \cdot \left\| (\nabla f_i(\bar{\theta}_t^i) - \frac{1}{N} \sum_{j=1}^N \nabla f_j(\bar{\theta}_t^j)) \odot \mathbf{1}_{\Omega_t} \right\|_\infty \\ &\leq |\lambda_2(\mathbf{W})|^{C_l} \cdot B/t, \end{aligned} \quad (93)$$

for some $B < \infty$ since the gradients are bounded.

For the second term in the right hand side of (92), we first apply the inequality $\|(N^{-1} \sum_{i=1}^N \nabla f_i(\bar{\theta}_t^i)) \odot (\xi_t^{-1} \mathbf{1}_{\Omega_t} - \mathbf{1})\|_\infty \leq \|N^{-1} \sum_{i=1}^N \nabla f_i(\bar{\theta}_t^i)\|_\infty \|(\xi_t^{-1} \mathbf{1}_{\Omega_t} - \mathbf{1})\|_\infty$ from [60]. Now, the probability that coordinate k is included is given by:

$$P(k \in \Omega_t) = 1 - P\left(\bigcap_{i=1}^N k \notin \Omega_{t,i}\right) = 1 - \left(1 - \frac{1}{d}\right)^{p_t N} = \xi_t, \quad (94)$$

and that $\mathbb{E}[\mathbf{1}_{\Omega_t}] = \xi_t \mathbf{1}$. Then, observing that each element in $\xi_t^{-1} \mathbf{1}_{\Omega_t}$ is bounded in $[0, \xi_t^{-1}]$ and applying the Hoeffding's inequality [61], the following holds true for all $x > 0$:

$$P(\|\xi_t^{-1} \mathbf{1}_{\Omega_t} - \mathbf{1}\|_\infty \geq x) \leq 2d \cdot e^{-2x^2/\xi_t^{-2}}, \quad (95)$$

where we have applied a union bound argument to take care of the ℓ_∞ -norm.

Setting $x = \xi_t^{-1} \sqrt{(\log(2dt^2) - \log \epsilon)/2}$ and applying another union bound show that with probability at least $1 - (\pi^2 \epsilon/6)$, the following holds for all $t \geq 1$:

$$\begin{aligned} & \left\| \frac{1}{N} \sum_{i=1}^N \nabla f_i(\bar{\theta}_t^i) \odot (\xi_t^{-1} \mathbf{1}_{\Omega_t} - \mathbf{1}) \right\|_\infty \\ & \leq \xi_t^{-1} \left\| \frac{1}{N} \sum_{i=1}^N \nabla f_i(\bar{\theta}_t^i) \right\|_\infty \sqrt{\frac{\log(2dt^2/\epsilon)}{2}}, \end{aligned} \quad (96)$$

As $d \gg 0$, we have $\xi_t^{-1} \approx d/(p_t N)$. Recalling $p_t \geq C_0 t$ yields the desired result in Lemma 3.

References

- [1] J. Lafond, H.-T. Wai, and E. Moulines, "D-FW: Communication Efficient Distributed Algorithms for High-dimensional Sparse Optimization," in *Proc ICASSP*, Mar 2016.
- [2] H.-T. Wai, A. Scaglione, J. Lafond, and E. Moulines, "A projection-free decentralized algorithm for non-convex optimization," in *Proc GlobalSIP*, December 2016.
- [3] V. Cevher, S. Becker, and M. Schmidt, "Convex Optimization for Big Data: Scalable, randomized, and parallel algorithms for big data analytics," *IEEE Signal Process. Mag.*, vol. 31, no. 5, pp. 32–43, Sep. 2014.
- [4] A. H. Sayed, S.-Y. Tu, J. Chen, X. Zhao, and Z. J. Towfic, "Diffusion strategies for adaptation and learning over networks: an examination of distributed strategies and network behavior," *IEEE Signal Process. Mag.*, vol. 30, no. 3, pp. 155–171, May 2013.
- [5] Z. Liu and L. Vandenberghe, "Interior-point method for nuclear norm approximation with application to system identification," *SIAM J. Matrix Anal. Appl.*, vol. 31, no. 3, pp. 1235–1256, 2010.
- [6] E. J. Candès and B. Recht, "Exact matrix completion via convex optimization," *Found. Comput. Math.*, vol. 9, no. 6, pp. 717–772, 2009.

- [7] C. Ravazzi, S. M. Fosson, and E. Magli, “Randomized algorithms for distributed nonlinear optimization under sparsity constraints,” *IEEE Trans. on Signal Process.*, vol. 64, no. 6, pp. 1420–1434, Mar 2016.
- [8] S. Patterson, Y. C. Eldar, and I. Keidar, “Distributed compressed sensing for static and time-varying networks,” *IEEE Trans. on Signal Process.*, vol. 62, no. 19, pp. 4931–4946, July 2014.
- [9] J. Tsitsiklis, “Problems in decentralized decision making and computation,” Ph.D. dissertation, Dept. of Electrical Engineering and Computer Science, M.I.T., Boston, MA, 1984.
- [10] A. G. Dimakis, S. Kar, J. M. F. Moura, M. G. Rabbat, and A. Scaglione, “Gossip Algorithms for Distributed Signal Processing,” *Proc. IEEE*, vol. 98, no. 11, pp. 1847–1864, Nov. 2010.
- [11] P. Bianchi and J. Jakubowicz, “Convergence of a multi-agent projected stochastic gradient algorithm for non-convex optimization,” *IEEE Trans. Autom. Control*, vol. 58, no. 2, pp. 391–405, Feb 2013.
- [12] I.-A. Chen, “Fast distributed first-order methods,” Master’s thesis, MIT, 2012.
- [13] G. Qu and N. Li, “Harnessing smoothness to accelerate distributed optimization,” *CoRR*, vol. abs/1605.07112, May 2016.
- [14] B. Johansson, T. Keviczky, M. Johansson, and K. H. Johansson, “Subgradient methods and consensus algorithms for solving convex optimization problems,” in *Proc. CDC*, Dec 2008, pp. 4185–4190.
- [15] S. Ram, A. Nedić, and V. Veeravalli, “Distributed stochastic subgradient projection algorithms for convex optimization,” *Journal of Optimization Theory and Applications*, vol. 147, no. 3, pp. 516–545, 2010.
- [16] W. Shi, Q. Ling, G. Wu, and W. Yin, “A proximal gradient algorithm for decentralized composite optimization,” *IEEE Trans. on Signal Process.*, vol. 63, no. 22, pp. 6013–6023, Nov 2015.
- [17] D. Jakovetic, J. Xavier, and J. M. F. Moura, “Fast distributed gradient methods,” *IEEE Trans. Autom. Control*, vol. 59, no. 5, pp. 1131–1146, May 2014.
- [18] A. Nedić, A. Olshevsky, and W. Shi, “Achieving geometric convergence for distributed optimization over time-varying graphs,” *CoRR*, vol. abs/1607.03218, July 2016.
- [19] X. Li and A. Scaglione, “Convergence and applications of a gossip based gauss newton algorithm,” *IEEE Trans. on Signal Process.*, vol. 61, no. 21, pp. 5231–5246, Nov 2013.
- [20] D. Varagnolo, F. Zanella, A. Cenedese, G. Pillonetto, and L. Schenato, “Newton-raphson consensus for distributed convex optimization,” *IEEE Trans. Autom. Control*, vol. 61, no. 4, pp. 994–1009, April 2016.
- [21] T.-H. Chang, A. Nedic, and A. Scaglione, “Distributed constrained optimization by consensus-based primal-dual perturbation method,” *IEEE Trans. Autom. Control*, vol. 59, no. 6, pp. 1524–1538, June 2014.

- [22] J. Duchi, A. Agarwal, and M. J. Wainwright, “Dual averaging for distributed optimization: Convergence analysis and network scaling,” *IEEE Trans. Autom. Control*, vol. 57, no. 3, pp. 592–606, March 2012.
- [23] E. Wei and A. Ozdaglar, “On the $o(1/k)$ convergence of asynchronous distributed alternating direction method of multipliers,” *CoRR*, vol. abs/1307.8254, July 2013.
- [24] A. Simonetto and H. Jamali-Rad, “Primal recovery from consensus-based dual decomposition for distributed convex optimization,” *JOTA*, vol. 168, no. 1, pp. 172–197, 2016.
- [25] M. Hong, “Decomposing linearly constrained nonconvex problems by a proximal primal dual approach: Algorithms, convergence, and applications,” *CoRR*, vol. abs/1604.00543, Apr 2016.
- [26] Y. Yang, G. Scutari, D. P. Palomar, and M. Pesavento, “A parallel stochastic approximation method for nonconvex multi-agent optimization problems,” *CoRR*, vol. abs/1410.5076, Oct 2014.
- [27] P. D. Lorenzo and G. Scutari, “Next: In-network nonconvex optimization,” *IEEE Trans. on Signal and Info. Process. over Networks*, 2016.
- [28] H.-T. Wai and A. Scaglione, “Consensus on state and time: Decentralized regression with asynchronous sampling,” *IEEE Trans. on Signal Process.*, vol. 63, no. 11, pp. 2972–2985, June 2015.
- [29] H.-T. Wai, T.-H. Chang, and A. Scaglione, “A consensus-based decentralized algorithm for non-convex optimization with application to dictionary learning,” in *Proc ICASSP*, Apr 2015, pp. 3546–3550.
- [30] M. Frank and P. Wolfe, “An algorithm for quadratic programming,” *Naval Res. Logis. Quart.*, 1956.
- [31] Z. Wu and K. Teo, “A conditional gradient method for an optimal control problem involving a class of nonlinear second-order hyperbolic partial differential equations,” *Journal of Mathematical Analysis and Applications*, vol. 91, no. 2, pp. 376 – 393, 1983.
- [32] M. Jaggi and M. Sulovsky, “A simple algorithm for nuclear norm regularized problems,” in *ICML*, June 2010.
- [33] A. Joulin, K. Tang, and L. Fei-Fei, “Efficient image and video co-localization with frank-wolfe algorithm,” in *ECCV*, Sept 2014.
- [34] L. Zhang, V. Kekatos, and G. B. Giannakis, “Scalable electric vehicle charging protocols,” *CoRR*, vol. abs/1510.00403v2, Oct 2016.
- [35] M. Fukushima, “A modified frank-wolfe algorithm for solving the traffic assignment problem,” *Transportation Research Part B: Methodological*, vol. 18, no. 2, pp. 169–177, April 1984.
- [36] M. Jaggi, “Revisiting Frank-Wolfe: Projection-free sparse convex optimization,” in *ICML*, June 2013.

- [37] S. Ghosh and H. Lam, “Computing worst-case input models in stochastic simulation,” *CoRR*, vol. abs/1507.05609, July 2015.
- [38] S. Lacoste-Julien, “Convergence rate of Frank-Wolfe for non-convex objectives,” *CoRR*, vol. abs/1607.00345, July 2016.
- [39] J. Lafond, H.-T. Wai, and E. Moulines, “On the online Frank-Wolfe algorithms for convex and non-convex optimizations,” *CoRR*, vol. abs/1510.01171v2, Aug 2016.
- [40] S. Ghadimi and G. Lan, “Accelerated gradient methods for nonconvex nonlinear and stochastic programming,” *Mathematical Programming*, vol. 156, no. 1, pp. 59–99, Feb 2015.
- [41] J. Duchi, S. Shalev-Shwartz, Y. Singer, and T. Chandra, “Efficient projections onto the ℓ_1 -ball for learning in high dimensions,” in *ICML*, July 2008.
- [42] G. H. Golub and C. F. van Loan, *Matrix computations*, 4th ed. Johns Hopkins University Press, Baltimore, MD, 2013.
- [43] A. Defazio, F. Bach, and S. Lacoste-Julien, “SAGA: A fast incremental gradient method with support for non-strongly convex composite objectives,” in *NIPS*, Dec 2014.
- [44] A. Scaglione, R. Pagliari, and H. Krim, “The decentralized estimation of the sample covariance,” in *Proc. Asilomar*, Nov. 2008, pp. 1722–1726.
- [45] Q. Ling, Y. Xu, W. Yin, and Z. Wen, “Decentralized low-rank matrix completion,” in *Proc ICASSP*, Mar 2012.
- [46] L. Mackey, A. Talwalkar, and M. I. Jordan, “Distributed matrix completion and robust factorization,” *Journal of Machine Learning Research*, vol. 16, pp. 913–960, 2015.
- [47] H.-F. Yu, C.-J. Hsieh, S. Si, and I. Dhillon, “Scalable coordinate descent approaches to parallel matrix factorization for recommender systems,” in *ICDM*. IEEE, 2012, pp. 765–774.
- [48] B. Recht and C. Ré, “Parallel stochastic gradient algorithms for large-scale matrix completion,” *Mathematical Programming Computation*, vol. 5, no. 2, pp. 201–226, 2013.
- [49] V. Chandrasekaran, S. Sanghavi, P. A. Parrilo, and A. S. Willsky, “Sparse and low-rank matrix decompositions,” in *Proc. Allerton*, 2009, pp. 962–967.
- [50] G. H. Mohimani, M. Babaie-Zadeh, and C. Jutten, “Fast Sparse Representation Based on Smoothed L0 Norm,” in *ICA*, ser. Lecture Notes in Computer Science. Springer, Sep. 2007, pp. 389–396.
- [51] L. Bako, “Identification of switched linear systems via sparse optimization,” *Automatica*, vol. 47, no. 4, pp. 668 – 677, 2011.
- [52] T. Blumensath and M. E. Davies, “Iterative hard thresholding for compressed sensing,” *CoRR*, vol. abs/0805.0510, May 2008.
- [53] M. E. Yildiz and A. Scaglione, “Coding with side information for rate-constrained consensus,” *IEEE Trans. on Signal Process.*, vol. 56, no. 8, pp. 3753–3764, Aug 2008.

- [54] H. Attiya and J. Welch, *Distributed Computing: Fundamentals, Simulations, and Advanced Topics*. Wiley, 2004.
- [55] L. Xiao and S. Boyd, “Fast linear iterations for distributed averaging,” *Systems & Control Letters*, vol. 53, no. 1, pp. 65–78, Sep. 2004.
- [56] F. M. Harper and J. A. Konstan, “The movielens datasets: History and context,” *ACM TiiS*, Jan 2015.
- [57] E. v. Berg, M. P. Friedlander, G. Hennenfent, F. Herrmann, R. Saab, and Ö. Yilmaz, “Sparco: A testing framework for sparse reconstruction,” Dept. Computer Science, University of British Columbia, Vancouver, Tech. Rep. TR-2007-20, October 2007.
- [58] B. P. Polyak, *Introduction to Optimization*. Optimization Software, Inc., 1987.
- [59] E. A. Nirminskii, “Convergence conditions for nonlinear programming algorithms,” *Cybernetics*, no. 6, pp. 79–81, Nov 1972.
- [60] R. A. Horn and C. R. Johnson, *Topics in matrix analysis*. Cambridge: Cambridge University Press, 1994, corrected reprint of the 1991 original.
- [61] P. Massart, *Concentration Inequalities and Model Selection*. Springer, 2003.